

ChaNoXity: The Nonlinear Dynamics of Nature

A. Sengupta

Department of Mechanical Engineering

Indian Institute of Technology Kanpur, Kanpur 208016, INDIA.

E-Mail: osegu@iitk.ac.in

Abstract

In this paper we employ the topological-multifunctional mathematical language and techniques of non-injective illposedness developed in Sengupta (2003) to formulate a notion of *ChaNoXity* — Chaos-Nonlinearity-Complexity — in describing the specifically nonlinear dynamical evolutionary processes of Nature. Non-bijective ill-posedness is the natural mode of expression for chanoxy that aims to focus on the nonlinear interactions generating dynamical evolution of real irreversible processes. The basic dynamics is considered to take place in a matter-antimatter *kitchen space* $X \times \mathfrak{X}$ of Nature that is inaccessible to both the functional matter (X) and multifunctional antimatter (\mathfrak{X}) components. These component spaces are distinguished by opposing evolutionary directional arrows and satisfy the defining property

$$(\forall A \subseteq X, \exists \mathfrak{A} \subseteq \mathfrak{X}) \text{ s.t. } (A \cup \mathfrak{A} = \emptyset).$$

Dynamical equilibrium is considered to be represented by such *competitively collaborating stasis* states of the matter-antimatter constituents of Nature.

1 Introduction

This paper applies the mathematical language and techniques of non-bijective, and in particular non-injective, ill-posedness developed in Sengupta (2003) to formulate an integrated approach to chaos, nonlinearity and complexity (ChaNoXity), where a complex system is taken to be characterized by

- ▶ a collection of many *interdependent parts*
- ▶ that interact with each other through *competitive nonlinear collaboration*
- ▶ leading to *emergent, self-organized behaviour*.¹

We will show how each of these defining characteristics of complexity can be described and structured within the mathematical framework of our multifunctional graphical convergence of a net of functions $(f)_\alpha$. In this programme, convergence in topological spaces continues to be our principal tool, and the particular topologies of significance that emerge are the topology of saturated sets and the A -exclusion topology, with A a subset of the domain of f_α . We will demonstrate that a complex system can be described as an association of independent

¹Competitive collaboration — as opposed to reductionism — in the context of this characterization is to be understood as follows: The interdependent parts retain their individual identities, with each contributing to the whole in its own characteristic fashion *within the framework of global properties of the union*. A comparison of reductionism as summarized in Figs. 6a, b, and c, shows that although the properties of the whole are generated by the parts, these units acting independently on their own cannot account for the emergent global behaviour of the whole.

expert groups, each entrusted with a specific specialized task by a top-level central coordinating command, that consolidates and regulates the inputs received from its different constituent units by harmonizing and combining them into an emerging whole; thus the complexity of a system, broadly speaking, is the amount of information needed to describe it. In this task, and depending on the evolving complexity of the dynamics, the central unit delegates its authority to subordinate units that report back to it the data collected at its own level of authority.

Recall that (i) a multifunction — which constitutes one of the foundational notions of our work — and the non-injective function are connected by

$$f \text{ is a non-injective function} \iff f^- \text{ is a multifunction} \quad (1)$$

$$f \text{ is a multifunction} \iff f^- \text{ is a non-injective function.}$$

and (ii) the neighbourhood of a point $x \in (X, \mathcal{U})$ — which is a generalization of the familiar notion of distances of metric spaces — is a nonempty subset N of X containing an open set $U \in \mathcal{U}$; thus $N \subseteq X$ is a neighbourhood of x iff $x \in U \subseteq N \subseteq (X, \mathcal{U})$ for some open set U of X . The collection of all neighbourhoods of x

$$\mathcal{N}_x \stackrel{\text{def}}{=} \{N \subseteq X : x \in U \subseteq N \text{ for some } U \in \mathcal{U}\} \quad (2)$$

is the neighbourhood system at x , and the subcollection U of \mathcal{U} used in this expression constitutes a neighbourhood (local) base or basic neighbourhood system, at x . The properties

- (N1) x belongs to every member N of \mathcal{N}_x ,
- (N2) The intersection of any two neighbourhoods of x is another neighbourhood of x : $N, M \in \mathcal{N}_x \Rightarrow N \cap M \in \mathcal{N}_x$,
- (N3) Every superset of any neighbourhood of x is a neighbourhood of x : $(M \in \mathcal{N}_x) \wedge (M \subseteq N) \Rightarrow N \in \mathcal{N}_x$

characterize \mathcal{N}_x completely and imply that a subset $G \subseteq (X, \mathcal{U})$ is open iff it is a neighbourhood of each of its points. Accordingly if \mathcal{N}_x is an arbitrary collection of subsets of X associated with each $x \in X$ satisfying (N1) – (N3), then the special class of neighbourhoods G

$$\mathcal{U} = \{G \in \mathcal{N}_x : x \in B \subseteq G \text{ for some } B \in \mathcal{N}_x \text{ and each } x \in G\} \quad (3)$$

defines a unique topology on X containing a basic neighbourhood B at each of its points x for which the neighbourhood system is the prescribed collection \mathcal{N}_x . Among the three properties (N1) – (N3), the first two now re-expressed as

- (NB1) x belongs to each member B of \mathcal{B}_x .
- (NB2) The intersection of any two members of \mathcal{B}_x contains another member of \mathcal{B}_x : $B_1, B_2 \in \mathcal{B}_x \Rightarrow (\exists B \in \mathcal{B}_x : B \subseteq B_1 \cap B_2)$.

are fundamental in the sense that the resulting subcollection \mathcal{B}_x of \mathcal{N}_x generates the full system by appealing to (N3). This basic neighbourhood system, or local base, at x in (X, \mathcal{U}) satisfies

$$\mathcal{B}_x \stackrel{\text{def}}{=} \{B \in \mathcal{N}_x : x \in B \subseteq N \text{ for each } N \in \mathcal{N}_x\} \quad (4)$$

which reciprocally determines the full neighbourhood system

$$\mathcal{N}_x = \{N \subseteq X : x \in B \subseteq N \text{ for some } B \in \mathcal{B}_x\} \quad (5)$$

as all the supersets of these basic elements.

The topology of saturated sets is defined in terms of equivalence classes $[x]_\sim = \{y \in X :$

$y \sim x \in X\}$ generated by a relation \sim on a set X ; the neighbourhood system \mathcal{N}_x of x in this topology consists of all supersets of the equivalence class $[x]_\sim \in X/\sim$. In the x -exclusion topology of all subsets of X that exclude x (plus X , of course), the neighbourhood system of x is just $\{X\}$. While the first topology provides, as in Sengupta (2003), the motive force for an evolutionary direction in time, the second will define an *anti-space* \mathfrak{X} of (associated with; generated by) X , with an oppositely directed evolutionary arrow. With *dynamic equilibrium* representing a state of stasis between the associated opposing motives of evolution, (*static*) *equilibrium* will be taken to mark the end of a directional evolutionary process represented by convergence of the associated sequence to an adherence set.

Let $f : X \rightarrow Y$ be a function and $f^- : Y \rightarrow X$ its multi-inverse: hence $ff^-f = f$ and $f^-ff^- = f^-$ although $f^-f \neq \mathbf{1}_X$ and $ff^- \neq \mathbf{1}_Y$ necessarily. Some useful identities for subsets $A \subseteq X$ and $B \subseteq Y$ are shown in Table 1, where the complement of a subset $A \subseteq X$ is denoted by $A^c = \{x : (x \in X - A) \wedge (x \notin A)\}$. Let the *f-saturation* $\mathcal{S}_f(A) := f^-f(A)$ of A and the *f-component* $\mathcal{C}_f(B) := ff^-(B) = B \cap f(X)$ of B on the image of f define generalizations of injective and surjective mappings in the sense that any f behaves one-one and onto on its saturated and component sets respectively, so that it is possible to replace each of the relevant assertions of Table 1 with the more direct injectivity and surjectivity conditions on f . Indeed

$$\begin{aligned} f(x) = y &\implies f(f^-f(x)) = y = ff^-(y) \\ &\implies f(\mathcal{S}_f(x)) = \mathcal{C}_f(y) \end{aligned}$$

and

$$\begin{aligned} x = f^-(y) &\implies f^-f(x) = x = f^-(ff^-(y)) \\ &\implies \mathcal{S}_f(x) = f^-(\mathcal{C}_f(y)) \end{aligned}$$

proves the bijectivity of $f : \mathcal{S}_f(x) \rightarrow \mathcal{C}_f(y)$ restricted to $\mathcal{S}_f(x)$ and $\mathcal{C}_f(y)$; hence in the bijective inverse notation the corresponding functional equation takes the form

$$f(\mathcal{S}_f(A)) = \mathcal{C}_f(B) \iff \mathcal{S}_f(A) = f^{-1}(\mathcal{C}_f(B)). \quad (6)$$

These important generalizations of the bijectivity of functions are of great value to us because our notion of chaos and complexity is based on ill-posedness of the non-bijective type of functional equations $f(x) = y$.

All statements of the first column of the table for saturated sets $A = \mathcal{S}_f(A)$ apply to the quotient map q ; observe that $q(A^c) = (q(A))^c$. Moreover combining the respective entries of both the columns, it is easy to verify the following results for the saturation map $\mathcal{S}_f = f$ on saturated sets $A = \mathcal{S}_f(A)$.

- (a) $\mathcal{S}_f(\bigcup A_i) = \bigcup \mathcal{S}_f(A_i)$: The union of saturated sets is saturated.
- (b) $\mathcal{S}_f(\bigcap A_i) = \bigcap \mathcal{S}_f(A_i)$: The intersection of saturated sets is saturated.
- (c) $X - \mathcal{S}_f(A) = \mathcal{S}_f(X - A)$: The complement of a saturated set is saturated.
- (d) $A_1 \subseteq A_2 \Rightarrow \mathcal{S}_f(A_1) \subseteq \mathcal{S}_f(A_2)$
- (e) $\mathcal{S}_f(\bigcap A_i) = \emptyset \Rightarrow \bigcap A_i = \emptyset$.

While properties (a) and (b) lead to the topology of saturated sets, the third makes it a complemented topology when the (closed) complement of an open set is also an open set. In this topology there are no boundaries between sets which are isolated in as far as a sequence eventually in one of them converging to points in the other is concerned.

Since the guiding incentive for this work is an understanding of the precise role of irre-

	$f: X \rightarrow Y$	$f^-: Y \rightarrow X$
1	$A_1 \subseteq A_2 \Rightarrow f(A_1) \subseteq f(A_2)$ $\Leftarrow \text{ iff } A = \mathcal{S}_f(A)$	$B_1 \subseteq B_2 \Rightarrow f^-(B_1) \subseteq f^-(B_2)$ $\Leftarrow \text{ iff } B = \mathcal{C}_f(B)$
2	$f(A) \subseteq B \Leftrightarrow A \subseteq f^-(B)$ $B \subseteq f(A) \Rightarrow f^-(B) \subseteq A \text{ iff } A = \mathcal{S}_f(A)$	$f(A) \subseteq B \Leftrightarrow A \subseteq f^-(B)$ $B \subseteq f(A) \Leftarrow f^-(B) \subseteq A \text{ iff } B = \mathcal{C}_f(B)$
3	$A = \emptyset \Leftrightarrow f(A) = \emptyset$	$f^-(\emptyset) = \emptyset$ $f^-(B) = \emptyset \Rightarrow B = \emptyset \text{ iff } B = \mathcal{C}_f(B)$
4	$f(A_1) \cap f(A_2) = \emptyset \Rightarrow A_1 \cap A_2 = \emptyset$ $\Leftarrow \text{ iff } A = \mathcal{S}_f(A)$	$f^-(B_1) \cap f^-(B_2) = \emptyset \Leftarrow B_1 \cap B_2 = \emptyset$ $\Rightarrow \text{ iff } B = \mathcal{C}_f(B)$
5	$f(\cup_\alpha A_\alpha) = \cup_\alpha f(A_\alpha)$	$f^-(\cup_\alpha B_\alpha) = \cup_\alpha f^-(B_\alpha)$
6	$f(\cap_\alpha A_\alpha) \subseteq \cap_\alpha f(A_\alpha)$, " = " iff $A = \mathcal{S}_f(A)$	$f^-(\cap_\alpha B_\alpha) = \cap_\alpha f^-(B_\alpha)$
7	$f(A^c) = (f(A))^c \cap f(X)$ iff $A = \mathcal{S}_f(A)$	$f^-(B^c) = ((f^-(B))^c$

Table 1: The role of saturated and component sets in a function and its inverse; here all $A = \mathcal{S}_f(A)$ and $B = \mathcal{C}_f(B)$ are to be understood to hold for every $A \subseteq X$ and $B \subseteq Y$. Unlike f , f^- preserves the basic set operations in the sense of 5, 6, and 7. This makes f^- rather than f the ideal instrument for describing topological and measure theoretic properties like continuity and measurability of functions.

versibility and nonlinearity in the dynamical evolution of irreversible real processes, we will propose an index of nonlinear irreversibility in essentially the kitchen space $X \times \mathfrak{X}$ of Nature, wherein all the evolutionary dynamics are postulated to take place. The real world X is only a projection of this multifaceted kitchen that is distinguished in having a non-real anti-component \mathfrak{X} interacting with X to generate the dynamical reality perceived in the later. This nonlinearity index, together with the dynamical stasis between opposing directional arrows associated with X and its anti-world \mathfrak{X} , suggests a description of time's arrow that, unlike both the historical and modern entropic approaches, is specifically nonlinear with chaos and complexity being the prime manifestations of strongly nonlinear systems.

The entropy produced within a system due to irreversibilities within it (Kondepudi and Prigogine, 1998) are generated by nonlinear dynamical interactions between the system and its anti-world, and the objective of this paper is to clearly define this interaction and focus on its relevance in the dynamical evolution of Nature.

2 ChaNoXity: Chaos-Nonlinearity-Complexity

2.1 Entropy, Irreversibility, and Nonlinearity

In this subsection we summarize the “modern” approach to entropy due to De Donder as enunciated by Kondepudi and Prigogine (1998) which explicitly incorporates irreversibility into the formalism of the Second Law of Thermodynamics thereby making it unnecessary to consider ideal, non-real, reversible processes for computing (changes in) entropy. This follows from the original Clausius inequality

$$dS \geq \frac{dQ}{T}$$

that may be written in the form

$$dS = \frac{dQ}{T} + dI \tag{7}$$

where dQ/T is due to the heat exchanged by the system with its exterior and I , the “uncompensated transformation” of Clausius, represents the entropy produced from the real irreversible processes occurring within the system. In postulating the existence of an entropy function $S(U, V, N)$ of the extensive parameters of internal energy U , volume V , and mole numbers $\{N_j\}_{j=1}^J$ of the chemical constituents comprising a composite system that is defined for all equilibrium states, we follow Callen (1985) in supposing that in the absence of internal constraints the extensive parameters assume such values that maximize S over all the constrained equilibrium states. The entropy of the composite system is additive over the constituent subsystems, and is continuous, differentiable, and increases monotonically with respect to the energy U . This last property implies that $S(U, V, N)$ can be inverted in $U(S, V, N)$; hence

$$dU(S, V, \{N_j\}) = \frac{\partial U}{\partial S} dS + \frac{\partial U}{\partial V} dV + \sum_{j=1}^J \frac{\partial U}{\partial N_j} dN_j \quad (8)$$

defines the *intensive parameters*

$$\frac{\partial U}{\partial S} \stackrel{\text{def}}{=} T(S, V, \{N_j\}_{j=1}^J), \quad V, \{N_j\} \text{ held const} \quad (9a)$$

$$\frac{\partial U}{\partial V} \stackrel{\text{def}}{=} -P(S, V, \{N_j\}_{j=1}^J), \quad S, \{N_j\} \text{ held const} \quad (9b)$$

$$\frac{\partial U}{\partial N_j} \stackrel{\text{def}}{=} \mu_j(S, V, \{N_j\}_{j=1}^J), \quad S, V \text{ held const} \quad (9c)$$

of absolute temperature T , pressure P , and chemical potential μ_j of the j^{th} component, from the macroscopic extensive ones. Inversion of Eq. (8) gives the differential *Gibbs entropy* definition

$$dS(U, V, \{N_j\}) \stackrel{\text{def}}{=} \frac{1}{T(U, V, \{N_j\})} dU + \frac{P(U, V, \{N_j\})}{T(U, V, \{N_j\})} dV - \sum_{j=1}^J \frac{\mu_j(U, V, \{N_j\})}{T(U, V, \{N_j\})} dN_j \quad (10)$$

providing an equivalent correspondence of the partial derivatives $(\partial S/\partial U)_{V, N_j} = 1/T(U, V, \{N_j\})$, $(\partial S/\partial V)_{U, N_j} = P(U, V, \{N_j\})/T$, and $(\partial S/\partial N_j)_{U, V} = -\sum_{j=1}^J \mu_j(U, V, \{N_j\})/T$ with the intensive variables of the system.

In the spirit of the Pfaffian differential form, dependence of the intensive variables of the First Law

$$\begin{aligned} dU(S, V, \{N_j\}) &= dQ(S, V, \{N_j\}) + dW(S, V, \{N_j\}) + dM(S, V, \{N_j\}), \\ &= dQ(S, V, \{N_j\}) - P(S, V, \{N_j\}) dV + \sum_{j=1}^J \mu_j(S, V, \{N_j\}) dN_j \end{aligned} \quad (11)$$

— that can be taken to define the heat flux dQ — on the respective extensive macroscopic variables U , V , or N_j serves to decouple the (possibly nonlinear) bonds between them; this is necessary and sufficient for the resultant thermodynamics to be classified as *quasi-static* or *reversible*. These ideal states as pointed out by Callen (1985) are simply an ordered class of equilibrium states, neutral with respect to time-reversal and without any specific directional properties, that is distinguished from natural real processes of ordered *temporal successions* of equilibrium and non-equilibrium states: *a reversible quasi-static process is simply a directionless collection of elements of an ordered set*.² From the definition Eq. (9a) of the absolute

²Jos Uffink (2001) delineates three different types of (ir)reversibilities. The most comprehensive among these follows from the notion of a *time-(a)symmetric theory* that requires the (non)existence of a reverse process

temperature T , it follows that *under quasi-static conditions*

$$dQ(S) \stackrel{\text{def}}{=} T(S) dS, \quad (12)$$

reduces the heat transfer dQ to formally behave work-like that permits Eq. (11) to be expressed in the *combined first and second law* form

$$dU(S, V, \{N_j\}) = T(S) dS - P(V) dV + \sum_{j=1}^J \mu(N_j) dN_j \quad (13a)$$

$$dS(U, V, \{N_j\}) = \frac{1}{T(U)} dU + \frac{P(V)}{T(U)} dV - \sum_{j=1}^J \frac{\mu(N_j)}{T(U)} dN_j \quad (13b)$$

which are just the integrable *quasi-static versions* of Eqs. (8, 10). Note that the total energy input and the corresponding entropy transfer in the quasi-static case reduces to a simple sum of the constituent parts of the change. For non quasi-static real processes, this linear superposition of the solution into its individual components is not justified as the solution of the resulting Pfaffian equation is the general $U(S, V, \{N_j\}_j = \text{const.}$. For any natural non-cyclic real process therefore, the identification

$$dQ(S, V, \{N_j\}) \stackrel{\text{def}}{=} T(S, V, \{N_j\}) dS \quad (14)$$

reduces (8) to the first law form (11) for real processes that no longer decomposes into individual and non-interacting heat, mechanical work, and mass transforming processes of its quasi-static counterpart (13a). Eq. (14) is graphically expressed (Kondepudi and Prigogine, 1998) in the spirit of (7) as

$$\begin{aligned} dS &= \frac{dQ(S, V, \{N_j\})}{T(S, V, \{N_j\})} \\ &= \frac{d\hat{Q}}{T} + \frac{d\tilde{Q}}{T} \\ &= d\hat{S} + d\tilde{S}, \end{aligned} \quad (15)$$

where the total entropy exchange is expressed as a sum of two parts: the first

$$d\hat{S} = \frac{d\hat{Q}}{T} \geq 0$$

may be positive, zero or negative depending on the specific nature of energy transfer $d\hat{Q}$ with the (infinite) exterior reservoir, but the second

$$d\tilde{S} = \frac{d\tilde{Q}}{T} \geq 0 \quad (16)$$

$\mathcal{P}_r := \{r(-t) : -t_f \leq t \leq -t_i\}$ for every permissible forward process $\mathcal{P} := \{s(t) : t_i \leq t \leq t_f\}$ of the theory; here $r = Rs$ with $R^2 = \mathbf{1}$, is the time-reversal of state s . Although in contrast with mechanics thermodynamics has no equations of motion, the Second Law endows it with a time-asymmetric character and a thermodynamic process is irreversible iff its reverse \mathcal{P}_r is not allowed by the theory.

Two weaker concepts of reversibility — requiring only that the system and its environment be restored to the respective initial conditions by the reverse process without any reference to the intermediate states, and quasi-staticity in which the process is poised so delicately as to proceed infinitely slowly, effectively in equilibrium throughout — are more common in thermodynamics. Our use of the notion of irreversibility in Sec. 2.2.1 will be in the spirit of time-irreversibility.

representing the entropy produced by irreversible nonlinear processes within the system is always positive. Expressing dQ by the first law Eq. (11) in terms of the basic macroscopic extensive variables U , V , and N , yields for a composite body $C = A \cup B$ of two parts A and B , each interacting with its own infinite reservoir under the constraint $U = U_A + U_B$, $V = V_A + V_B$ and $N = N_A + N_B$, the Gibbs expression

$$dS_C(U, V, N) = \left[\frac{1}{T_A} dU_A + \frac{1}{T_B} dU_B \right] + \left[\frac{p_A}{T_A} dV_A + \frac{p_B}{T_B} dV_B \right] - \left[\frac{\mu_A}{T_A} dN_A + \frac{\mu_B}{T_B} dN_B \right] \quad (17)$$

for the entropy exchanged by C in reaching a state of *static equilibrium* with its infinite environment; here T , P and μ are the parameters of the reservoirs that completely determine the internal state of C . This exchange of energy with the surroundings perturbs the system from its state of equilibrium and sets up internal irreversible nonlinear processes between the two subsystems, driving C towards a new state of *dynamic equilibrium* that can be represented (Katchalsky and Curran (1965), Kondepudi and Prigogine (1998)) in terms of flows of extensive quantities set up by forces generated by the intensive variables. Thus for a composite *dynamically* interacting system $C = A \cup B$ consisting, for example, of two chambers A and B of volumes V_A and V_B containing two nonidentical gases at distinct temperatures, pressures, and mole numbers, the entropy generated by nonlinear irreversible processes within the system when the partition separating the chambers is removed, can be expressed in the Gibbs form as

$$\begin{aligned} d\widetilde{S}_C(U, V, N) &= \left[\frac{1}{T_A} - \frac{1}{T_B} \right] dU_A + \left[\frac{p_A}{T_A} - \frac{p_B}{T_B} \right] dV_A - \left[\frac{\mu_A}{T_A} - \frac{\mu_B}{T_B} \right] dN_A, \\ U &= U_A + U_B = \text{const}, \quad V = V_A + V_B = \text{const}, \quad N = N_A + N_B = \text{const} \end{aligned} \quad (18)$$

with each term on the right, a product of an intensive thermodynamic force driving the corresponding extensive thermodynamic flow, contributing to the *uncompensated heat* of Clausius, see Kondepudi and Prigogine (1998). This uncompensated heat generated entirely within the system due to the nonlinear irreversible dynamical interactions between A and B is taken to be responsible for the increase of entropy accompanying all natural processes. This interaction between two (finite) systems is to be compared and contrasted with the static interaction between a (finite) system and an (infinite) reservoir. Compared with the later for which the time evolution is unidirectional with the system unreservedly acquiring the properties of the reservoir that undergoes no perceptible changes leading to a state of *static equilibrium* as a result of the *passive interaction* of the system with its reservoir, the system-system interaction is fundamentally different as it evolves bidirectionally such that the properties of the composite are not of either of the subsystems, but an average of the individual properties defining an eventual state of *dynamic interactive equilibrium*. This distinction between passive and dynamical interactive equilibria resulting respectively from the uni- and bi-directional interactions is clearly revealed in Eqs. (17) and (18), with bi-directionality of the later being displayed by the *difference form of the generalized forces*. Accordingly, subsystem A (respectively subsystem B) has two directional arrows imposed on it: the first from its own forward evolution that is opposed by a second reverse process due to its interactive interaction with B (respectively A), see Fig. 3. Evolution requires all macroscopic extensive variables — and hence all the related microscopic intensive parameters — to be functions of time so that equilibrium, in the case of Eq. (18) for example, demands

$$\frac{d\widetilde{S}_C}{dt} = 0 \implies \left(\frac{dU_A}{dt} = 0 \right) \wedge \left(\frac{dV_A}{dt} = 0 \right) \wedge \left(\frac{dN_A}{dt} = 0 \right)$$

$$\iff (T_A(t) = T_B(t)) \wedge (p_A(t) = p_B(t)) \wedge (\mu_A(t) = \mu_B(t)). \quad (19)$$

While we return to this topic subsequently using the tools of directed sets and convergence in topological spaces, for the present it suffices to note that for an emerging, complex, self-organizing, evolving system of the type that concerns us here, the linear reductionist decoupling of its entropy change into two independent parts, one with the exterior and the other the consequent internal generation as given by Eq. (15), is difficult to justify as these constitute a system of interdependent evolutionary interlinked processes, depending on each other for their sustenance and contribution to the whole. Thus, “life” forms in which $d\widehat{S}$, arising from the energy exchanged as food and other sustaining modes with the exterior, is completely dependent on the capacity $d\widetilde{S}$ of the life to utilise this exchange, which in turn depends on, and is regulated by $d\widehat{S}$. These interdependent, non-reductionist, contributions of constituent parts to the whole is a direct consequence of nonlinearity that effectively implies $f(\alpha x_1 + \beta x_2) \neq \alpha f(x_1) + \beta f(x_2)$ for the related processes. The second “non-life” example requires the change to be determined by such internal parameters as mass, specific heat and chemical concentration of the constituents parts. Thus, for example, in the adiabatic mixing of a hot and cold body A and B the equilibrium temperature, given in terms of the respective mole numbers N , specific heat c and temperature T , by

$$N_A c_A (T_A - T) = N_B c_B (T - T_B) \quad (20)$$

sets up a state of dynamical equilibrium in which the bi-directional evolutionary arrow prevents A from annihilating B with the equilibrium condition $T = T_A$, $P = P_A$, $\mu = \mu_A$. Putting the heat balance equation in the form

$$dQ_A + (-dQ_B) = 0, \quad dQ = NcdT$$

suggests that the heat transfer out of a body, considered as a negative real number, be treated as the additive inverse to the positive transfers into the system. This sets up a one-to-one correspondence between the forward and its associated reverse directional naturally occurring real process that evolves to a state of dynamic equilibrium.

The noteworthy feature of this evolutionary thermodynamics — based entirely on (linear) differential calculus — is that it reduces the dynamics, as in Eqs. (8) and (10), to a separation of its governing macroscopic extensive variables, and it is relevant to investigate the extent to which this decoupling of the motive forces responsible for the evolution is indeed justifiable for the strongly nonlinear, self-organizing and emerging complex dynamical systems of nature³.

³The following extracts from the remarkably explicit lecture MIT-CTP-3112 by Michel Baranger (2000), delivered possibly in 2000/2001, are worth recalling . “Chaos is still not part of the American university’s physics curriculum; most students get physics degrees without ever hearing about it. The most popular textbook in classical mechanics does not include chaos. Why is that? The answer is simple. Physicists did not have the time to learn chaos, because they were fascinated by something else. That something else was 20th century physics of relativity, quantum mechanics, and their myriad of consequences. Chaos was not only unfamiliar to them; it was slightly distasteful!”

In offering an explanation for this, Baranger argues that in discovering Calculus, Newton and Leibnitz “provided the scientific world with the most powerful new tool since the discovery of numbers themselves. The idea of calculus is simplicity itself. Smoothness (of functions) is the key to the whole thing. There are functions that are not smooth …”. The discovery of calculus led to that of Analysis and “after many decades of unbroken success with analysis, theorists became imbued with the notion that all problems would eventually yield to it, given enough effort and enough computing power. If you go to the bottom of this belief you find the following. *Everything* can be reduced to little pieces, therefore everything can be known and understood, if we analyze it to a fine enough scale. The enormous success of calculus is in large part responsible for the decidedly reductionist attitude of most twentieth century science, the belief in absolute control arising from detailed knowledge.”

Nonetheless, “chaos is the anti-calculus revolution, it is the rediscovery that calculus does not have infinite power. Chaos is the collection of those mathematical truths that have nothing to do with calculus. Chaos theory

Such a separation of variables tacitly implies, as in the example considered above, that the total energy exchange taking place when the gases are allowed to mix completely is separable into independent parts arising from changes in temperature and volume, or from diffusion and mixing of the gases, *with none of them having any effect on the others*. Recalling that the basic property of a complex system that serves to define its “complex” character is the interdependence of its interacting parts responsible for non-reductionism, this contrary implication of independence of the extensive parameters directly conflicts with the notions of chaos and complexity.

The objective of this paper is to propose an explicitly nonlinear, topological formulation of dynamical evolution in an integrated *chanoxity* — chaos, nonlinearity, complexity — form that focuses on nonlinearity generating self-organization, adaption, and emergence.

2.2 Maximal Noninjectivity is Chaos

Chaos was defined in Sengupta (2003) as representing maximal non-injective ill-posedness in the temporal evolution of a dynamical system and was based on the purely set theoretic arguments of Zorn’s Lemma and Hausdorff Maximal Chain Theorem. It was, however, necessary to link this with topologies because evolutionary directions are naturally represented by adherence and convergence of the associated nets and filters, and this require topologies for describing their eventual and frequenting behaviour. For this we found the topology of saturated sets generated by the increasingly non-injective evolving maps (leading thereby to maximality of ill-posedness and hence to chaos) to provide the motivation for maximal non-injectivity that in turn leads to the concept of the ininality of topologies generated by a function $f : X \rightarrow Y$ which is simultaneously image and preimage continuous. In this case, the topologies on the range $\mathcal{R}(f)$ and domain $\mathcal{D}(f)$ of f are locked with respect to each other as far as further temporal evolution of f is concerned by having the respective topologies defined as the f -images in Y of f^- -saturated open sets of X . Thus equation (6), taken with $U = \mathcal{S}_e(U)$ and $\mathcal{C}_q(V) = V$ that are simple consequences of the definitions

$$\text{IT}\{e; \mathcal{V}\} \stackrel{\text{def}}{=} \{U \subseteq X : U = e^-(V), V \in \mathcal{V}\} \quad (21)$$

and

$$\text{FT}\{\mathcal{U}; q\} \stackrel{\text{def}}{=} \{V \subseteq Y : q^-(V) = U, U \in \mathcal{U}\} \quad (22)$$

of initial and final topologies, defines for some $V \in \mathcal{V}$ a subset $U \in \mathcal{U}$ satisfying

$$e^-ee^-(V) = e^-(V) \stackrel{\text{IT}}{=} U = e^-e(U) \iff (U = \mathcal{S}_e(U)) \wedge (e(U) = \mathcal{C}_e(V)), \quad (23a)$$

while for a subset $A \subseteq U \in \mathcal{U}$ such that $\mathcal{S}_q(A) = U$, the topology \mathcal{V} of Y as

$$q^-q(A) = U \stackrel{\text{FT}}{=} q^-(V) = q^-(qq^-(V)) \iff (V = \mathcal{C}_q(V)) \wedge (q(U) = V) \quad (23b)$$

because $qq^- = \mathbf{1}_Y$ on $\mathcal{R}(q)$; see also column 2, row 1 of Table 1. As these equations show, preimage and image continuous functions are not necessarily open functions: a preimage continuous function is open iff $e(U)$ is an open set in Y and an image continuous function is open iff the saturation of every open set of X is also an open set. The generation of new topologies on the domain and range of a function — these will generally be quite different from the original topologies the spaces might have possessed — by the evolving dynamics of increasingly

solves a wide variety of scientific and engineering problems which do not respond to calculus.”

nonlinear maps is a basic property of the evolutionary process that constitutes the motive for such dynamical changes. Putting these equations together, we get

$$U, V \in \text{IFT}\{\mathcal{U}; f; \mathcal{V}\} \iff (\mathcal{U} = \{f^-(V)\}_{V \in \mathcal{V}}) \wedge (\{f(U)\}_{U \in \mathcal{U}} = \mathcal{V}), \quad (24a)$$

which reduces to

$$U, V \in \text{HOM}\{\mathcal{U}; f; \mathcal{V}\} \iff (\mathcal{U} = \{f^{-1}(V)\}_{V \in \mathcal{V}}) \wedge (\{f(U)\}_{U \in \mathcal{U}} = \mathcal{V}) \quad (24b)$$

for a open-continuous bijection f satisfying both $\mathcal{S}_f(A) = A$, $\forall A \subseteq X$ and $\mathcal{C}_f(B) = B$, $\forall B \subseteq Y$. Observe that the only difference between Eqs. (24a) and (24b) lies in the one-one and onto character of f .

There are two defining components, temporal and spatial, in any natural evolutionary processes. However, these are mathematically equivalent in the sense that both can be represented as pre-ordered sets with the additional directional property of a *directed set* (\mathbb{D}, \preceq) which satisfies

- (DS1) $\alpha \in \mathbb{D} \Rightarrow \alpha \preceq \alpha$ (that is \preceq is reflexive)
- (DS2) $\alpha, \beta, \gamma \in \mathbb{D}$ such that $(\alpha \preceq \beta \wedge \beta \preceq \gamma)$ implies $\alpha \preceq \gamma$ (that is \preceq is transitive)
- (DS3) For all $\alpha, \beta \in \mathbb{D}$, there exists a $\gamma \in \mathbb{D}$ such that $\alpha \preceq \gamma$ and $\beta \preceq \gamma$

with respect to the *direction* \preceq . While the first two properties are obvious and constitutes the preordering of \mathbb{D} , the third replaces antisymmetry of an order with the condition that every pair of elements of \mathbb{D} always has a successor. This directional property of \mathbb{D} , that imparts to the static pre-order a sequential arrow by allowing it to choose a path of progress between various alternatives that exists when non-comparable elements bifurcate the arrow, will be used to model evolutionary processes in space and time. Besides the obvious examples \mathbb{N} , \mathbb{R} , \mathbb{Q} , or \mathbb{Z} of totally ordered sets, more exotic instances of directed sets imparting directions to neighbourhood systems in X tailored to the specific needs of convergence theory are summarized in Table 2, where $\beta \in \mathbb{D}$ is the directional index.

Directed set \mathbb{D}	Direction \preceq induced by \mathbb{D}
$\mathbb{D}N = \{N : N \in \mathcal{N}_x\}$	$M \preceq N \Leftrightarrow N \subseteq M$
$\mathbb{D}N_t = \{(N, t) : (N \in \mathcal{N}_x)(t \in N)\}$	$(M, s) \preceq (N, t) \Leftrightarrow N \subseteq M$
$\mathbb{D}N_\beta = \{(N, \beta) : (N \in \mathcal{N}_x)(x_\beta \in N)\}$	$(M, \alpha) \leq (N, \beta) \Leftrightarrow (\alpha \preceq \beta) \wedge (N \subseteq M)$

Table 2: Natural directions in (X, \mathcal{U}) induced by some useful directed sets of convergence theory. Significant examples of directed sets that are only partially ordered are $(\mathcal{P}(X), \subseteq)$, $(\mathcal{P}(X), \supseteq)$; $(\mathcal{F}(X), \subseteq)$, $(\mathcal{F}(X), \supseteq)$; $(\mathcal{N}_x, \subseteq)$, $(\mathcal{N}_x, \supseteq)$ for a set X . We take \mathcal{N}_x , suitably redefined if necessary, to be always a system of nested subsets of X .

While the neighbourhood system $\mathbb{D}N$ at a point $x \in X$ with the *reverse inclusion* direction \preceq is the basic example of natural direction of the neighbourhood system \mathcal{N}_x of x , the more relevant directed sets $\mathbb{D}N_t$ and $\mathbb{D}N_\beta$ are more convenient in convergence theory because unlike the first, these do not require a simultaneous application of the Axiom of Choice to every $N \in \mathcal{N}_x$.

Chaos as manifest in the limiting adhering attractors is a direct consequence of the increasing nonlinearity of the map under increasing iterations and with the right conditions, appears to be the natural outcome of the characteristic difference between a function f and its multiinverse f^- . Equivalence classes of fixed points stable and unstable, as generated by the saturation operator

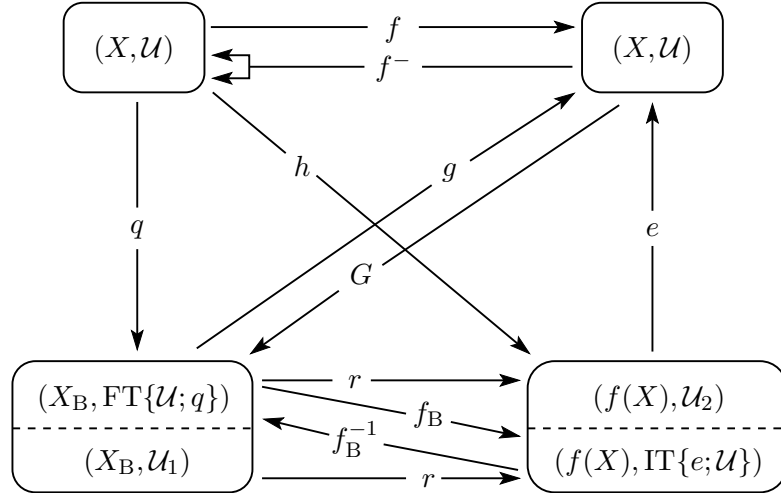


Figure 1: Generation of a multifunctional inverse $x = f^-(y)$ of the functional equation $f(x) = y$ for $f: X \rightarrow X$; here $G: Y \rightarrow X_B$ is a generalized inverse of f because $fGf = f$ and $GfG = G$ that follows from the commutativity of the diagrams. g and h are the injective and surjective restrictions of f ; these will be topologically denoted by their generic notations e and q respectively.

$\mathcal{S}_f = f^-f$, determine the ultimate behaviour of an evolving dynamical system, and since the eventual (as also frequent) nature of a filter or net is dictated by topology on the set, chaoticity on a set X leads to a reformulation of the open sets of X to equivalence classes generated by the evolving map f . In the limit of infinite iterational evolution in time of f resulting in the multifunction Φ , the generated open sets constitute a basis for a topology on $\mathcal{D}(f)$ and the basis for the topology of $\mathcal{R}(f)$ are the corresponding Φ -images of these equivalent classes. From the preceding discussions it follows that the motivation behind the forward evolution of a dynamical system leading to chaos is the drive toward a state of the dynamical system that supports ininality of the limit multi Φ^4 . In the limit of infinite iterations therefore, the open sets of the range $\mathcal{R}(f) \subseteq X$ are the multi images that graphical convergence generates at each of these inverse-stable fixed points. As readily verified from Fig. 1, X has two topologies imposed on it by the dynamics of f : the first of equivalence classes generated by the limit multi Φ in the domain of f and the second as Φ -images of these classes in the range of f . Hence while subdiagrams $X - (X_B, \text{FT}\{\mathcal{U}; q\}) - (f(X), \mathcal{U}_2)$ and $(X_B, \mathcal{U}_1) - (f(X), \text{IT}\{e; \mathcal{U}\}) - X$ apply to the final and initial topologies of X_B and $f(X)$ respectively, their superposition $X - (X_B, \text{FT}\{\mathcal{U}; q\}) - (f(X), \text{IT}\{e; \mathcal{U}\}) - X$ under the additional requirement of a homeomorphic f_B leads to the conditions $\mathcal{U}_1 = \text{IT}\{g; \mathcal{U}\}$ and $\mathcal{U}_2 = \text{FT}\{\mathcal{U}; h\}$ that X_B and $f(X)$ must possess. For this to be possible,

$$\begin{aligned} \text{FT}\{\mathcal{U}; q\} &= \text{IT}\{g; \mathcal{U}\} \\ \text{IT}\{e; \mathcal{U}\} &= \text{FT}\{\mathcal{U}; h\} \end{aligned}$$

⁴For the logistic map $f_\lambda(x) = \lambda x(1 - x)$ with chaos setting in at $\lambda = \lambda_* = 3.5699456$, this drive in ininality implies an evolution toward values of the spatial parameter $\lambda \geq \lambda_*$; this is taken to be a spatial parameter as it determines the degree of surjectivity of f_λ . Together with the temporal evolution in increasing noninjectivity for any λ , this comprises the full evolutionary dynamics of the logistic map. These two distinct dynamical mechanisms of increasing ontone and increasing noninjectivity are not independent, however. Thus λ — which we identify later as representing energy exchanges of all possible types that the system can have with the surroundings — determines the nature of the internal forward-backward stasis that leads to the eventual equilibrium of the system with its environment.

requires the image continuous q and the preimage continuous e to be also be open maps which translates to the ininality of f on (X, \mathcal{U}) , and hence for the topology of X to be simultaneously the direct and inverse images of itself under f . Recalling that the map f and the topology \mathcal{U} of X are already provided, this is interpreted to mean that the increasing nonlinear ill-posedness of the time-iterates of f is driven by ininality of the maximally ill-posed limit relation Φ on X^2 . In this case Φ acts as a non-bijective open and continuous relation such that the sequence of evolving functional relations (f^n) on X eventually behaves, by Eq. (6), homeomorphically on the saturated open sets of equivalence classes and their f^n -images in X . We define the resulting ininal topology on X to be the *chaotic topology on X associated with f* . Neighbourhoods of points in this topology cannot be arbitrarily small as they consist of all members of the equivalence class to which any element belongs; hence a sequence converging to any of these elements necessarily converges to all of them, and the eventual objective of chaotic dynamics is to generate a topology in X (irrespective of the original \mathcal{U}) with respect to which elements of the space can be grouped together in large equivalence classes in the sense that if a net converges simultaneously to points $x \neq y \in X$ then $x \sim y$: x is of course equivalent to itself while x, y, z are equivalent to each other iff they are simultaneously in every open set where the net may eventually be in. This hall-mark of chaos leads to a necessary eradication of any separation property that the space might have originally possessed.

The generation of a new topology on X by the dynamics of f on X is a consequence of the topology of pointwise biconvergence \mathcal{T} defined on the set of relations $\text{Multi}((X, \mathcal{U}), (Y, \mathcal{V}))$, (Sengupta, 2003). This generalization of the topology of pointwise convergence defines neighbourhoods of f in $\text{Multi}((X, \mathcal{U}), (Y, \mathcal{V}))$ to consist of those functions in $(\text{Multi}((X, \mathcal{U}), (Y, \mathcal{V})), \mathcal{T})$ whose images at any point $x \in X$ lie not only close enough to $f(x) \in Y$ (this gives the usual pointwise convergence) but additionally whose inverse images at $y = f(x)$ contain points arbitrarily close to x . Thus the graph of f must not only lie sufficiently close to $f(x)$ at x in $V \in \mathcal{V}$, but must also be such that $f^-(y)$ has at least one branch in the open set $U \in \mathcal{U}$ about x . This requires all members of a neighbourhood \mathcal{N}_f of f to “cling to” f as the number of points on the graph of f increases with the result that unlike for simple pointwise convergence, no gaps in the graph of the limit relation is possible not only on the domain of f but on its range too.

For any given integer $I \geq 1$, the open sets of $(\text{Multi}(X, Y), \mathcal{T})$ are

$$B((x_i), (V_i); (y_i), (U_i)) = \{g \in \text{Map}(X, Y) : \\ (g(x_i) \in V_i) \wedge (g^-(y_i) \cap U_i \neq \emptyset), i = 1, 2, \dots, I\}, \quad (25)$$

where $(x_i)_{i=1}^I \in X$, $(y_i)_{i=1}^I \in Y$, $(U_i)_{i=1}^I \in \mathcal{U}$ ($V_i)_{i=1}^I \in \mathcal{V}$ are chosen arbitrarily with reference to $(x_i, f(x_i))$. A local base at f , for $(x_i, y_i) \in \text{Graph}(f)$, is the set of functions of (25) with $y_i = f(x_i)$, and the collection of all local bases $B_\alpha = B((x_i)_{i=1}^{I_\alpha}, (V_i)_{i=1}^{I_\alpha}; (y_i)_{i=1}^{I_\alpha}, (U_i)_{i=1}^{I_\alpha})$, for every choice of $\alpha \in \mathbb{D}$, is a base ${}_T\mathcal{B}$ of $(\text{Multi}(X, Y), \mathcal{T})$; note that in this topology $(\text{Map}(X, Y), \mathcal{T})$ is a subspace of $(\text{Multi}(X, Y), \mathcal{T})$. The basic technical tools needed for describing the adhering limit relation in $(\text{Multi}(X, Y), \mathcal{T})$ is the algebraic concept of a filter which is a collection of subsets of X satisfying

- (F1) The empty set \emptyset does not belong to \mathcal{F} ,
- (F2) The intersection of any two members of a filter is another member of the filter: $F_1, F_2 \in \mathcal{F} \Rightarrow F_1 \cap F_2 \in \mathcal{F}$,
- (F3) Every superset of a member of a filter belongs to the filter: $(F \in \mathcal{F}) \wedge (F \subseteq G) \Rightarrow G \in \mathcal{F}$; in particular $X \in \mathcal{F}$,

and is generated by a subfamily $(B_\alpha)_{\alpha \in \mathbb{D}} = {}_T\mathcal{B} \subseteq \mathcal{F}$ of itself, known as the filter-base, characterized by

(FB1) There are no empty sets in the collection ${}_F\mathcal{B}$: $(\forall \alpha \in \mathbb{D})(B_\alpha \neq \emptyset)$

(FB2) The intersection of any two members of ${}_F\mathcal{B}$ contains another member of ${}_F\mathcal{B}$: $B_\alpha, B_\beta \in {}_F\mathcal{B} \Rightarrow (\exists B \in {}_F\mathcal{B}: B \subseteq B_\alpha \cap B_\beta)$.

Hence any family of subsets of X that does not contain the empty set and is closed under finite intersections is a base for a unique filter on X , and the filter-base

$${}_F\mathcal{B} \stackrel{\text{def}}{=} \{B \in \mathcal{F}: B \subseteq F \text{ for each } F \in \mathcal{F}\} \quad (26)$$

determines the filter

$$\mathcal{F} = \{F \subseteq X: B \subseteq F \text{ for some } B \in {}_F\mathcal{B}\} \quad (27)$$

as all the supersets of these basic elements. Note that the filter is an algebraic concept without any topological content; in order to be able to use it for the purely topological needs of convergence, a comparison of (F1)-(F3) and (FB1)-(FB2) with (N1)-(N3) and (NB1)-(NB2) of Sec. 1 show that the neighbourhood system \mathcal{N}_x at x is the *neighbourhood filter at x* and that any local base at x is a filter-base for \mathcal{N}_x : generally for any subset A of X , $\{N \subseteq X: A \subseteq \text{Int}(N)\}$ is a filter on X at A . All subsets of X containing a point $p \in X$ is the *principal filter* ${}_F\mathcal{P}(p)$ on X at p . More generally, the collection of all supersets of a nonempty subset A of X is the principal filter ${}_F\mathcal{P}(A) = \{N \subseteq X: A \subseteq \text{Int}(N)\}$ at A . The singleton sets $\{\{x\}\}$ and $\{A\}$ are particularly simple examples of filter-bases that generate the principal filters at $\{x\}$ and A ; other useful examples that we require subsequently are the set of all residuals

$$\text{Res}(\mathbb{D}) = \{\mathbb{R}_\alpha: \mathbb{R}_\alpha = \{\beta \in \mathbb{D}: \beta \succeq \alpha \in \mathbb{D}\}\}$$

of a directed set \mathbb{D} , and the neighbourhood systems \mathcal{B}_x and \mathcal{N}_x . By adjoining the empty set to this filter gives the p -inclusion and A -inclusion topologies on X respectively.

The utility of filters in describing convergence in topological spaces arises from fact that a filter \mathcal{F} on X can always be associated with the net $\chi_{\mathcal{F}}: {}_{\mathbb{D}}F_x \rightarrow X$ defined by

$$\chi_{\mathcal{F}}(F, x) \stackrel{\text{def}}{=} x \quad (28)$$

where ${}_{\mathbb{D}}F_x = \{(F, x): (F \in \mathcal{F})(x \in F)\}$ is a directed set with direction $(F, x) \preceq (G, y) \Rightarrow (G \subseteq F)$; reciprocally a net $\chi: \mathbb{D} \rightarrow X$ corresponds to the filter-base

$${}_F\mathcal{B}_\chi \stackrel{\text{def}}{=} \{\chi(\mathbb{R}_\alpha): \text{Res}(\mathbb{D}) \rightarrow X \text{ for all } \alpha \in \mathbb{D}\}, \quad (29)$$

with the corresponding filter \mathcal{F}_χ being obtained by taking all supersets of the elements of ${}_F\mathcal{B}_\chi$. Filters and their bases are extremely powerful tools for maximal non-injective ill-posedness in the context of the algebraic Hausdorff Maximal Principle and Zorn's Lemma⁵, that we summarize below.

Let f be a noninjective map in $\text{Multi}(X)$ and $\mathcal{I}(f)$ be the number of injective branches of f ; let

$$F = \{f \in \text{Multi}(X): f \text{ is a noninjective function on } X\} \in \mathcal{P}(\text{Multi}(X))$$

be the collection of all noninjective functions such that

⁵**Hausdorff Maximal Principle (HMP):** Every partially ordered set has a maximal chain.

Zorn's Lemma: Every inductive set has at least one maximal element.

A partially ordered set X is said to be *inductive* if every chain of X has an upper bound in X .

(1) For every α in a directed set \mathbb{D} , F has the extension property

$$(\forall f_\alpha \in F)(\exists f_\beta \in F): \mathcal{I}(f_\alpha) \leq \mathcal{I}(f_\beta).$$

Define a partial order \preceq on $\text{Multi}(X)$ for $f_\alpha, f_\beta \in \text{Map}(X) \subseteq \text{Multi}(X)$ by

$$\mathcal{I}(f_\alpha) \leq \mathcal{I}(f_\beta) \iff f_\alpha \preceq f_\beta, \quad (30)$$

with $\mathcal{I}(f) := 1$ for the smallest f denote a partial ordering $(\text{Multi}(X), \preceq)$ of $\text{Multi}(X)$. This is actually a preorder on $\text{Multi}(X)$ in which all function with the same number of injective branches are equivalent to each other. Observe that $\text{Multi}(X)$ has two orders imposed on it: the first \preceq between its elements f , and the second the usual \subseteq that orders subsets of these functional elements.

(2) Let

$$C_\nu = \{f_\alpha \in \text{Multi}(X): f_\alpha \preceq f_\nu\} \in \mathcal{P}(\text{Multi}(X)), \quad \nu \in \mathbb{D}, \quad (31)$$

be chains of non-injective functions where $f_\alpha \in F$ is to be identified with the iterates f^i , the number of injective branches $\mathcal{I}(f)$ depending on i . The chains are built from the smallest C_0 , the domain \mathcal{D} of f , by application of a choice function g_C that generates the immediate successor

$$C_j := g(C_i) = C_i \cup g_C(\mathcal{G}(C_i) - C_i) \in \mathcal{X}$$

of C_i by picking one from the many

$$\mathcal{G}(C_i) = \{f \in F - C_i: \{f\} \cup C_i \in \mathcal{X}\}$$

that C_i may possibly possess; here

$$\mathcal{X} = \{C \in \mathcal{P}(F): C \text{ is a chain in } (\text{Multi}(X), \preceq)\} \in \mathcal{P}^2(\text{Multi}(X)) \quad (32)$$

is the collection of all chains in $\text{Multi}(X)$ with respect to the order (30). Applying g to C_0 n -times produces the chain $C_n = \{\mathcal{D}, f(\mathcal{D}), \dots, f^n(\mathcal{D})\}$, and the smallest common chain

$$\begin{aligned} \mathcal{C} &= \{C_j \in \mathcal{P}(\text{Multi}(X)): C_i \subseteq C_k \text{ for } i \leq k\} \subseteq \mathcal{X} \\ &= \{\mathcal{D}, \{\mathcal{D}, f(\mathcal{D})\}, \{\mathcal{D}, f(\mathcal{D}), f^2(\mathcal{D})\}, \dots\} \quad C_0 := \mathcal{D} \end{aligned} \quad (33)$$

of all the possible g -towered chains $\{C_i\}_{i=0,1,2,\dots}$ of $\text{Multi}(X)$ constitutes a principal filter of totally ordered subsets of $(\text{Multi}(X), \subseteq)$ at C_0 . Notice that while $\mathcal{X} \in \mathcal{P}^2(\text{Multi}(X))$ is a set of sets, $C \in \mathcal{P}(\text{Multi}(X))$ is relatively simpler as a set of elements of $f \in \text{Multi}(X)$, which at the base level of the tree of interdependent structures of $\text{Multi}(X)$, is canonically the simplest.

To continue further with the application of Hausdorff Maximal Principle to the partially ordered set (\mathcal{X}, \preceq) of sets, it is necessary that

- (a) There exists a smallest element C_0 in \mathcal{X} with no predecessor,
- (b) Every element $C \in \mathcal{X}$ has an immediate successor $g(C)$ in \mathcal{X} such that there is no element of \mathcal{X} lying strictly between C and $g(C)$, and
- (c) \mathcal{X} is an *inductive* set in the sense that every chain \mathcal{C} of (\mathcal{X}, \preceq) has a supremum $\sup_{\mathcal{X}}(\mathcal{C}) = \cup_{C \in \mathcal{C}} C$ in \mathcal{X} , see footnote 5.

Any subset \mathcal{T} of \mathcal{X} satisfying these conditions is often graphically referred to as a *tower*; \mathcal{X} is of course a tower by definition. The intersection of all possible towers of \mathcal{X} is the towered chain \mathcal{C} of \mathcal{X} , Eq. (33). Criterion (c) above is especially crucial as it effectively disqualifies

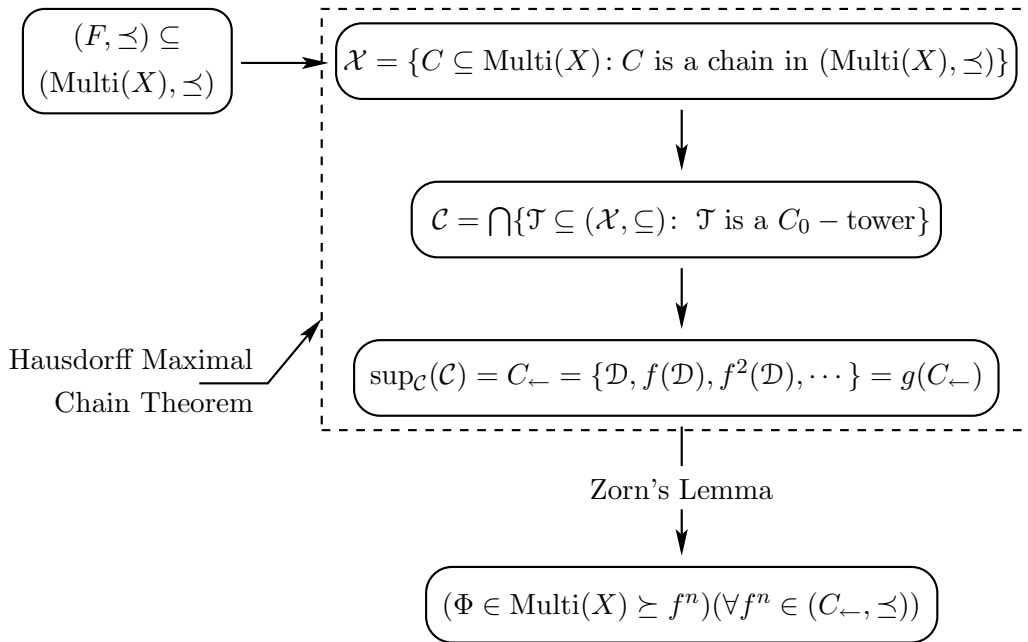


Figure 2: Application of Zorn’s Lemma to a partially ordered set $F = \{f \in \text{Multi}(X) : f \text{ is a noninjective function}\}$. $\mathcal{C} = \{\mathcal{D}, \{\mathcal{D}, f(\mathcal{D})\}, \{\mathcal{D}, f(\mathcal{D}), f^2(\mathcal{D})\}, \dots\}$ is a chain of towered chains of *functions* in $\text{Multi}(X)$ with $C_0 = \mathcal{D}$, the domain of f . Notice that to obtain a maximal Φ at the base level $\text{Multi}(X)$, it is necessary to go two levels higher: $\mathcal{X} \in \mathcal{P}^2(\text{Multi}(X)) \rightarrow C \in \mathcal{P}(\text{Multi}(X)) \rightarrow \Phi \in \text{Multi}(X)$ is a three-tiered structure with the two-tiered HMP feeding to the third of Zorn’s Lemma.

(F, \preceq) as a likely candidate for HMP: the supremum of the chains of increasingly non-injective functions need not be a *function*, but is likely to be a multifunction. Hence \mathcal{X} in the conditions above is the space of relations, and it is necessary to consider C of Eq. (31) as a subset of this $\text{Multi}(X)$ rather than of F . The careful reader cannot fail to note that the induction of $\text{Multi}(X)$ effectively leads to an “extension” of $\text{Map}(X)$ to the set of arbitrary relations wherein the supremum of the chain of non-injective functions may possibly lie. However it must be realized that in this purely algebraic setting without topologies on the sets, the supremum constitutes only a static cap on the family of equilibrium ordered states: the chains being only ordered and not directed are devoid of any dynamical evolutionary character.

(3) Application of the Hausdorff Maximal Principle to (\mathcal{X}, \subseteq) now yields

$$\begin{aligned} \sup_{\mathcal{C}}(\mathcal{C}) &= C_↔ = \{f_\alpha, f_\beta, f_\gamma, \dots\} \\ &= \{\mathcal{D}, f(\mathcal{D}), f^2(\mathcal{D}), \dots\} = g(C_↔) \in \mathcal{C} \end{aligned} \quad (34)$$

as the supremum of \mathcal{C} in \mathcal{C} , defined as a fixed-point of the tower generator g , without any immediate successor. Identification of this fixed-point supremum as one of the many possible maximal elements of (\mathcal{X}, \subseteq) completes the application of Hausdorff Principle, yielding $C_↔$ as the required maximal chain of (\mathcal{X}, \subseteq) .

The technique of HMP is noteworthy because it presents a graphic step-wise algorithmic rule leading to an equivalent filter description and the algebraic notion of a *chained tower*. Not possessing any of the topological directional properties associated with a net or sequence, the tower comprises an ideal mathematical vocabulary for an ordered succession of equilibrium states of a quasi-static, reversible, process. The directional attributes of convergence and adherence

must be externally imposed on towered filters like \mathcal{C} by introducing the neighbourhood system: a filter \mathcal{F} converges to $x \in (X, \mathcal{U})$ iff $\mathcal{N}_x \subseteq \mathcal{F}$.

(4) Returning to the partially ordered set $(\text{Multi}(X), \preceq)$, Zorn's Lemma applied to the maximal chained element C_{\leftarrow} of the inductive set \mathcal{X} finally yields the required maximal element $\Phi \in \text{Multi}(X)$ as an upper bound of the maximal chain $(C_{\leftarrow}, \preceq)$. Because this limit need not in general be a function, the supremum does not belong to the towered chain having it as a fixed point, and may be considered as a contribution of the inverse functional relations (f_{α}^-) in the following sense. From Eq. (1), the net of increasingly non-injective functions of Eq. (30) implies a corresponding net of decreasingly multivalued functions ordered inversely by the relation $f_{\alpha} \preceq f_{\beta} \Leftrightarrow f_{\beta}^- \preceq f_{\alpha}^-$. Thus the inverse relations which are as much an integral part of graphical convergence as are the direct relations, have a smallest element belonging to the multifunctional class. Clearly, this smallest element as the required supremum of the increasingly non-injective tower of functions defined by Eq. (30), serves to complete the significance of the tower by capping it with a “boundary” element that can be taken to bridge the classes of functional and non-functional relations on X .

Having been assured of the existence of a largest element $\Phi \in \text{Multi}(X)$, we now proceed to construct it topologically. Let $(\chi_i := f^i(A))_{i \in \mathbb{N}}$ for a subset $A \subseteq X$ that we may take to be the domain of f , correspond to the ordered sequence (30). Using the notation of Eq. (29), let the totality of the sequences $\chi(\mathbb{R}_i) = \bigcup_{j \geq i} f^j(A)$ for each $i \in \mathbb{N}$ generate the decreasingly nested filter-base

$$\begin{aligned} {}_F\mathcal{B} &\stackrel{\text{def}}{=} \left\{ \bigcup_{j \geq i} f^j(A) \right\}_{i \in \mathbb{N}} \\ &= \left\{ \bigcup_{j \geq i} f^j(x) \right\}_{i \in \mathbb{N}} \quad \forall x \in A, \end{aligned} \tag{35}$$

corresponding to the sequence of functional iterates $(f^j)_{j \geq i \in \mathbb{N}}$. The existence of a maximal chain with a maximal element guaranteed by the Hausdorff Maximal Principle and Zorn's Lemma respectively implies a nonempty core of ${}_F\mathcal{B}$. We now identify this filterbase with the neighbourhood base at Φ and thereby define

$$\begin{aligned} \Phi(A) &\stackrel{\text{def}}{=} \text{adh}({}_F\mathcal{B}) \\ &= \bigcap_{i \geq 0} \text{Cl}(A_i), \quad A_i = \{f^i(A), f^{i+1}(A), \dots\} \end{aligned} \tag{36}$$

as the attractor of A , where the closure is with respect to the topology of pointwise bi-convergence induced by the neighbourhood filter base ${}_F\mathcal{B}$. Clearly the attractor as defined here is the graphical limit of the sequence of functions $(f^i)_{i \in \mathbb{N}}$ with respect to the directed sets of Table 2. This attractor represents, in the product space $X \times X$, the converged limit of the bi-directional evolutionary dynamics occurring in the kitchen space $X \times \mathfrak{X}$ (the *anti-space* $(\mathfrak{X}, \mathcal{U}_{\ominus})$ of (X, \mathcal{U}) is defined below) that induces the observable image $\Phi(A)$ in X . The antispace is not directly observable, being composed of *anti-elements* \mathfrak{x} that correspond in an unique, one-to-one fashion to the corresponding defining observables $x \in X$, just as the negative reals — which are not physically directly observable either — are attached in a one-to-one fashion with their corresponding defining positive counterparts in the manner

$$r + (-r) = 0, \quad r \in \mathbb{R}_+. \tag{37}$$

The anti-space is necessary for understanding the bi-directional evolutionary process responsible for a stasis of dynamic equilibrium of two sub-systems competitively collaborating with each other. The basic example of an anti-space is that of the negative reals with a *forward* direction

in the sense of the *decreasing* negatives resulting from an *exclusion anti-topology* \mathcal{U}_\ominus which is generated by the topology \mathcal{U} of the observable positive reals R_+ . This generalization of the additive inverse of the real number system to sets is considered in the next subsection.

2.2.1 The Antispace of a topological space

Postulate 1. The anti-set \mathfrak{X} .⁶ Let X be a set and suppose that for every $x \in X$ there exists an $\mathfrak{x} \in \mathfrak{X}$ with the property that

$$\mathfrak{X} \stackrel{\text{def}}{=} \{\mathfrak{x}: \{x\} \cup \{\mathfrak{x}\} = \emptyset\} \quad (38a)$$

defines the *anti-set* (also to be referred to as the *anti-image*) of X . This means that for every subset A of X there is an anti-set $\mathfrak{A} \subseteq \mathfrak{X}$ associated with (generated by) it such that

$$A \cup \mathfrak{B} \stackrel{\text{def}}{=} A - B, \quad B \longleftrightarrow \mathfrak{B}, \quad (38b)$$

implies $A \cup \mathfrak{A} = \emptyset$. Hence anti-sets of X act as *inhibitors* or *moderators* of X .

As compared with the directed set $(\mathcal{P}(X), \subseteq)$ that induces the natural direction of *decreasing subsets* of Table 2, the direction of *increasing supersets* induced by $(\mathcal{P}(X), \supseteq)$ — which understandably finds no ready application in convergence theory — is useful in generating an anti-topology \mathcal{U}_\ominus on \mathfrak{X} corresponding to the topology \mathcal{U} in X as follows. Let (x_0, x_1, x_2, \dots) be a sequence in X converging to $x_* \in X$ with reference to any of the reverse inclusion, forward direction, of decreasing neighbourhood system \mathcal{N}_{x_*} of Table 2, and consider the backward direction induced at the limit x_* by the directed set $(\mathcal{P}(X), \supseteq)$ of increasing supersets containing x_* . As the reverse sequence $(x_*, \dots, x_{i+1}, x_i, x_{i-1}, \dots)$ does not converge to x_0 unless it is eventually in every neighbourhood of this initial point, we employ the closed-open subsets

$$N_i - N_j = \begin{cases} (N_i - N_j) \cap N_i, & (\text{open}) \\ (N_i - N_j) \cap (X - N_j) & (\text{closed}) \end{cases} \quad (39)$$

($j > i$) in the *inclusion topology* of X with $x_i \in N_i - N_{i+1}$, $N_i \in \mathcal{N}_{x_*}$, to generate a topology in \mathfrak{X} in Postulate 2 below. For this, recall that while the *x-inclusion topology* of X comprise all subsets of X that *include* x (together with \emptyset) with the neighbourhood system \mathcal{N}_x being just these non-empty subsets of X , the *x-exclusion topology* are all those subsets $\mathcal{P}(X - \{x\})$ of X that *exclude* x (together with X), with $\{X\}$ and $\{\{y\}\}$ being its neighbourhood systems at x and any $y \neq x$. Thus while a net trivially converges to x in its exclusion topology, it converges to any other point $y \neq x$ iff it is eventually constant at $\{y, y, y, \dots\}$ ⁷. Since the open sets of the second of Eq. (39) in the x_* -exclusion topology are actually closed with respect to the inclusion topology, and arbitrary (respectively finite) union of open (respectively closed) sets belong to their respective classes, we postulate with respect to the directed set $\mathbb{D}N_i = \{(N_i, i): (N_i \in \mathcal{N}_{x_*})(x_i \in N_i)\}$ of Table 2 and a sequence $(x_i)_{i \geq 0}$ in (X, \mathcal{U}) converging to $x_* = \text{adh}_{i \geq 0}(\text{Cl}(N_i)) \in X$, that

Postulate 2. The anti-topology \mathcal{U}_\ominus . There exists a *decreasing* sequence of moderating anti-elements $(\mathfrak{x}_i)_{i < \infty}$ in \mathfrak{X} that converges to \mathfrak{x}_0 in the x_* -exclusion topology \mathcal{U}_\ominus of \mathfrak{X} generated by the closed sets $\{N_i - N_{i+1}\}_{i \geq 0}$ of (X, \mathcal{U}) , by being eventually constant in the open set $\mathfrak{N}_0 - \mathfrak{N}_1 \in \mathcal{U}_\ominus$ with value \mathfrak{x}_0 ; alternatively, all distinct points of these open sets of \mathcal{U}_\ominus are

⁶Anti-sets will be denoted by fraktur letters.

⁷I thank Joseph Lo for his clarifications on the subtleties of the exclusion topology, Private Communication, May 2004.

equivalent with respect to the converging sequences. Since the only manifestation of anti-sets in the observable real world is their inhibitory property, the *decreasing* sequence $(\mathfrak{x}_i)_{i<\infty}$ will be taken to converge to \mathfrak{x}_0 in $(\mathfrak{X}, \mathcal{U}_\ominus)$ if and only if the *increasing* sequence $(x_i)_{i\geq 0}$ converges in (X, \mathcal{U}) , that is if and only if the moderating sequence $(\dots, \mathfrak{x}_{(j+1)}, \mathfrak{x}_j, \mathfrak{x}_{(j-1)}, \dots, \mathfrak{x}_0)$ of \mathfrak{X} is eventually in every \mathcal{U}_\ominus -neighbourhood of \mathfrak{x}_0 as generated by the \mathcal{U} -closed, x_* -*exclusion* open sets, $\{N_i - N_{i+1}\}_{i\geq 0}$ of X . This decreasing *natural forward direction* in $(\mathfrak{X}, \mathcal{U}_\ominus)$ of Table 3 is to be compared with the *natural reverse directions* in (X, \mathcal{U}) , Table 2.

Directed set \mathbb{D}	Direction \preceq induced by \mathbb{D}
$\mathbb{D}\mathfrak{N} = \{\mathfrak{N}: \mathfrak{N} \in \mathcal{N}_\mathfrak{x}\}$	$\mathfrak{M} \preceq \mathfrak{N} \Leftrightarrow \mathfrak{M} \subseteq \mathfrak{N}$
$\mathbb{D}\mathfrak{N}_t = \{(\mathfrak{N}, t): (\mathfrak{N} \in \mathcal{N}_\mathfrak{x})(t \in \mathfrak{N})\}$	$(\mathfrak{M}, \mathfrak{s}) \preceq (\mathfrak{N}, t) \Leftrightarrow \mathfrak{M} \subseteq \mathfrak{N}$
$\mathbb{D}\mathfrak{N}_\beta = \{(\mathfrak{N}, \beta): (\mathfrak{N} \in \mathcal{N}_\mathfrak{x})(\mathfrak{x}_\beta \in \mathfrak{N})\}$	$(\mathfrak{M}, \alpha) \leq (\mathfrak{N}, \beta) \Leftrightarrow (\alpha \preceq \beta) \wedge (\mathfrak{M} \subseteq \mathfrak{N})$

Table 3: Natural forward directions in the antispace $(\mathfrak{X}, \mathcal{U}_\ominus)$ is to be compared with Table 2 of the natural reverse directions in (X, \mathcal{U}) . The direction of anti-events in \mathfrak{X} is opposite to that of X in the sense that the temporal sequence of images of events in X opposes that in \mathfrak{X} and the order of occurrence of events induced by the anti-world appear to be reversed to the real observer stationed in X .

Although the backward sequence $(x_i)_{i=\dots, i+1, i, i-1, \dots}$ in (X, \mathcal{U}) does not converge, the effect of the containing sequence $(\mathfrak{x}_i)_{i<\infty}$ of \mathfrak{X} on X is to inhibit the evolution of the forward sequence $(x_i)_{i\geq 0}$ to an effective state of dynamical stasis of equilibrium. It is to be noted that the uni-directional forward arrow $(\mathfrak{x}_*, \dots, \mathfrak{x}_2, \mathfrak{x}_1, x_0, x_1, x_2, \dots, x_*)$ powered by ininality in the composite real-anti world, translates into the bidirectionally of Eq. (38b) responsible for the dynamical stasis. The significance of these concepts can be appreciated by considering for X and \mathfrak{X} the sets of positive and negative reals, and for x_* , \mathfrak{x}_* a positive real number and its negative inverse image.

An open set of X is by definition a subset in which a net must eventually reside in order to converge to a point in that set. The existence of an anti-element $x \leftrightarrow \mathfrak{x}$ in \mathfrak{X} for every $x \in X$ requires all forward *increasing* directions in X to have a matching forward *decreasing* direction in \mathfrak{X} that actually *appears increasing forward when viewed from X* . It is this opposing complimentary inhibitory effects of \mathfrak{X} forward decreasing sequences on X — responsible by Eq. (38b) for moderating the normal uni-directional evolution in X — that leads to a stasis of dynamical balance between the opposing forces generated in the composite of a system with its environment. Obviously, the evolutionary process will cease when the opposing influences in X due to itself and that generated by its inhibitor \mathfrak{X} balance each other which is the state of dynamic equilibrium.

It should be noted that the moderating image \mathfrak{X} of X needs to be endowed with inverse inhibitory properties if (38b) is to be meaningful which leads to the separation properties of the conjugate spaces (X, \mathcal{U}) and $(\mathfrak{X}, \mathcal{U}_\ominus)$ shown in Table 4. It is significant that the anti-space is topologically distinguished in having its sequences converge with respect to increasing neighbourhoods of the limit point, a property that leads as already pointed out earlier to the existence of a multiplicity of equivalent limits in large neighbourhoods of \mathfrak{x}_0 to which the sequence in \mathfrak{X} converges, even when (X, \mathcal{U}) is Hausdorff. We conjecture, in the context of iterational evolution of functions that concerns us here, that the function-multiplication asymmetry of (1) introduced by the non-injectivity of the iterates is directly responsible for the difference in the separation properties of \mathcal{U} and \mathcal{U}_\ominus , which in turn prohibits the system from annihilating B

Property	(X, \mathcal{U})	$(\mathfrak{X}, \mathcal{U}_\ominus)$
T_0	$(\forall x \neq y \in X) (\exists N \in \mathcal{N}_x : N \cap \{y\} = \emptyset) \vee (\exists M \in \mathcal{N}_y : M \cap \{x\} = \emptyset)$	$(\forall \mathfrak{x} \neq \mathfrak{y} \in \mathfrak{X}) (\exists \mathfrak{N} \in \mathcal{N}_{\mathfrak{x}} : \mathfrak{N} \cap \{\mathfrak{y}\} = \emptyset) \vee (\exists \mathfrak{M} \in \mathcal{N}_{\mathfrak{y}} : \mathfrak{M} \cap \{\mathfrak{x}\} = \emptyset)$
T_1	$(\forall x \neq y \in X) (\exists N \in \mathcal{N}_x : N \cap \{y\} = \emptyset) \wedge (\exists M \in \mathcal{N}_y : M \cap \{x\} = \emptyset)$	$(\forall \mathfrak{x} \neq \mathfrak{y} \in \mathfrak{X}) (\exists \mathfrak{N} \in \mathcal{N}_{\mathfrak{x}} : \mathfrak{N} \cap \{\mathfrak{y}\} = \emptyset) \wedge (\exists \mathfrak{M} \in \mathcal{N}_{\mathfrak{y}} : \mathfrak{M} \cap \{\mathfrak{x}\} = \emptyset)$
T_2	$(\forall x \neq y \in X) (\exists N \in \mathcal{N}_x \wedge M \in \mathcal{N}_y : (M \cap N = \emptyset))$	$(\forall \mathfrak{x} \neq \mathfrak{y} \in \mathfrak{X}) (\exists \mathfrak{N} \in \mathcal{N}_{\mathfrak{x}} \wedge \mathfrak{M} \in \mathcal{N}_{\mathfrak{y}} : (\mathfrak{M} \cap \mathfrak{N} = \emptyset))$

Table 4: Comparison of the separation properties of (X, \mathcal{U}) and its inhibiting anti-space $(\mathfrak{X}, \mathcal{U}_\ominus)$.

mentioned earlier and forces it to adopt the forward-backward stasis of dynamic equilibrium. Recalling that non-injectivity of one-dimensional maps translate to pairs of injective branches with *positive* and *negative* slopes, we argue in the context of Fig. 4 that whereas branches with positive slope represent matter, those with negative slope correspond to anti-matter by Eq. 38b.

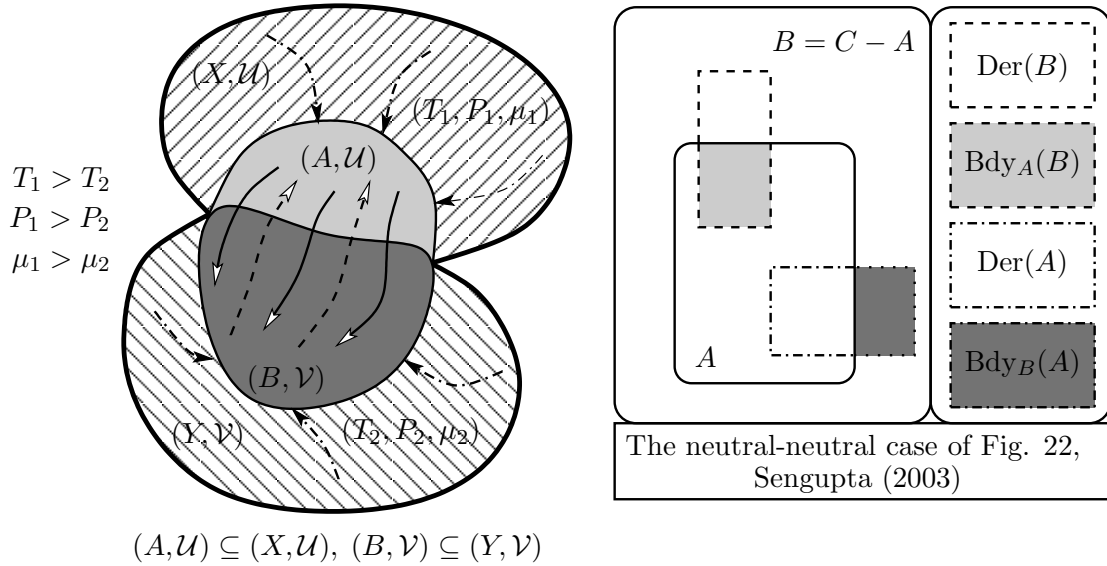


Figure 3: Schematic representation of irreversible entropy generation in $C = A \cup B$ with respect to the universe $X \cup Y$. The irreversible process is indicated by the nets of full arrows with open heads from A to B representing transfer of energy, volume, or mass driven by appropriate evolutionary directed set of a thermodynamic force (for instance due to a temperature gradient $T_1 > T_2$ inducing energy transfer) that provides the driving impetus of ininality for the directional transport. The dashed open arrows show the reverse evolution in C due to its inhibitor \mathfrak{C} , where $C \cup \mathfrak{C} = \emptyset$. The dash-dot arrows stand for the uni-directional transfer of energy from a reservoir that continues till the respective parts of C acquire the characteristics of their reservoirs. We shall identify the solid arrows in C with second law entropic emergence and the dashed arrows as anti-entropic self-organization.

As an example of the application of these ideas, let us return to Eqs. (17) and (18) for the entropy change due to external exchange and non-linear, irreversible, internal generation respectively. The external exchange of energy with the environment leads to a change in the internal state of the system which is then utilized in performing irreversible useful work relative to the environment. The situation is conveniently displayed in terms of the *neutral-neutral*

convergence mode of a net schematically represented in Fig. 3 and adapted from Fig. 22 of Sengupta (2003), illustrating the irreversible internal generation of entropy in a universe $C = A \cup B$, where A and B are two parts of a system prepared at different initial conditions as shown in the figure. In order to examine these questions in the evolutionary perspective, we first formalize the notion of

Definition. Interaction between two spaces. A space (A, \mathcal{U}) will be said to *interact* with a *disjoint* space (B, \mathcal{V}) if there exists a function f on the *sum space* (C, \mathcal{W}) , where $C = A \cup B$ and

$$\begin{aligned}\mathcal{W} &= \{W := U \cup V : (U \in \mathcal{U}) \wedge (V \in \mathcal{V})\} \\ &= \{W \subseteq C : (W \cap A \text{ is open in } A) \wedge (W \cap B \text{ is open in } B)\},\end{aligned}$$

which evolves graphically to a well defined limit relation in the topology of pointwise biconvergence on (C, \mathcal{W}) . The function f will be said to be an *interaction* between A and B .⁸

The forward evolution in (C, \mathcal{W}) motivated by the inducement of an ininal topology on C is opposed by the restraining, inhibiting, and backward influence arising from the exclusion topologies of the antispace

$$(\mathfrak{C}, \mathcal{W}_\ominus) = (\mathfrak{A} \cup \mathfrak{B}, \mathcal{U}_\ominus \cup \mathcal{V}_\ominus),$$

with the equivalence classes generated in the anti-space being responsible for the multiinverses of the evolving f that characterises the nonlinear state of C following the internal preparation of the system. This irreversible process is indicated in Fig. 3 by the nets of open-headed full arrows from (A, \mathcal{U}) to (B, \mathcal{V}) representing transfer of energy, volume, or mass driven by an appropriate evolutionary directed set of a thermodynamic force (for instance due to a temperature gradient $T_A > T_B$ inducing the energy transfer) that provides the driving impetus for directional transport motivated by ininality.

Since physical evolution powered by changes in the internal intensive parameters is represented by convergence of appropriate sequences and nets, it is postulated in keeping with the role of ininality, that equilibrium in uni-directional temporal evolutions like $X \rightarrow A \subseteq X$ or $Y \rightarrow B \subseteq Y$ sets up A and B as subspaces of X and Y respectively. For bi-directional processes like $A \leftrightarrow B$, the open headed dashed arrows of Fig. 3 from B to A represent the inhibiting backward influence of $(\mathfrak{C}, \mathcal{W}_\ominus)$ on (C, \mathcal{W}) . The assumptions

(a) Both the subsets A and B of C are perfect in the sense that $A = \text{Der}(A)$ and $B = \text{Der}(B)$ so that all points of each of these sets can be reached by sequences eventually in them, and

(b) $\text{Bdy}_B(A) = B$ and $\text{Bdy}_A(B) = A$ which enables all points of A and B to be directly accessed as limits by sequences in B and A ,

imply that any exchange of energy from the environment $E = X \cup Y$ to system C will be evenly dispersed through it by the irreversible, internal evolution of the system, once C attains equilibrium with E and is allowed to evolve unperturbed thereafter. This *global homogenizing principle of detailed balance*, applicable to evolutionary processes at the micro-level provides a rationale for equilibration in nature that requires every forward direct process to be balanced by an oppositely directed arrow, leading to the global equilibrium of thermodynamics. If backward

⁸If A and B are not disjoint, then this construction of the sum may not work because A and B will generally induce distinct topologies on C ; in this case \mathcal{W} is obtained as follows. Endow the disjoint copies $A_1 := A \times \{1\}$ and $B_2 := B \times \{2\}$ of A and B with topologies $\mathcal{U}_1 = \{U \times \{1\} : U \in \mathcal{U}\}$ and $\mathcal{V}_2 = \{V \times \{2\} : V \in \mathcal{V}\}$, which are homeomorphic with their originals with $a \mapsto (a, 1)$ and $b \mapsto (b, 2)$ being the respective homeomorphisms. Then $C = A_1 \cup B_2$ is the sum of A_1 and B_2 with the topology $\mathcal{W} = \{W \subseteq C : W = (U \times \{1\}) \cup (V \times \{2\}) : (U \in \mathcal{U}) \wedge (V \in \mathcal{V})\}$ inducing the subspaces (A_1, \mathcal{U}_1) and (B_2, \mathcal{V}_2) .

influences exactly balance the inducing forward impetus resulting in a complete restoration of all the intermediate stages, then the resulting *reversible process* is actually quasi-static with no effective changes; note that nontrivial equilibrated stasis cannot be generated by any reversible processes. Rather than subscribing to the additive (linear) decomposition of an environmental uni-directional energy exchange and the attendant bi-directional internal evolution implied by Eq. (15), we instead adopt the point of view that these processes are interrelated and the drive toward ininality is accompanied by its subsequent internal utilization, gainfully or otherwise with dissipation. In this sense, interaction will always imply the couple (f, \mathfrak{f}) of a function f and its anti-self \mathfrak{f} rather than f alone.

With reference to evolution of maps like the logistic $f_\lambda = \lambda x(1 - x)$, which for a particular λ can be taken to represent the subspace $C \subseteq E$ at equilibrium with its environment E , evolutionary changes in λ induce changes in the internal intensive thermodynamic parameters that follow uni-directional exchanges of C with E . This perturbs the equilibrium between components A and B resulting in further evolutionary iterational interaction between them. The forward iterational evolution of f_λ is hindered by the backward restraining effect of \mathfrak{C} which suppresses the continual increase of noninjectivity of f_λ that would otherwise lead to a state of maximum noninjective ill-posedness for this λ . Measurable global equilibrium represents a balance between the opposing induced local evolutionary forces that are determined by, and which in turn determine, the degree of energy exchange λ . The eventual ininality at $\lambda = 4$ represents continual energy absorption from E that is dissipated for the globalizing uniformity of Figs. 4 and 7a(c). For $3 < \lambda \leq \lambda_* = 3.5699456$ the energy input is gainfully employed to generate the complex structures that are needed to sustain the process at that level of λ .

Recalling footnote 4, we now summarize the principal features of the nonlinear evolutionary dynamics following interaction of a composite system with its surroundings.

(a) If the state of dynamic equilibrium of a composite system $C = A \cup B$ with its surroundings, as represented by the logistic map is disturbed by some form of communication between the two, forces are set up between the components A and B so as to absorb the effect of this disturbance.

(b) The consumption of the effects of this exchange is motivated by a *simultaneous*, non-reductionist drive towards increasing surjectivity *and* increasing noninjectivity of the map f_λ and its evolved iterated images, which eventually leads to a state of maximal non-injectivity on the domain of f . Owing to the function-multiplication asymmetry of the map, such a condition would signify static equilibrium and an end to all further evolutionary processes, a state of dissipative annihilation, burn-out and ininality.

(c) Since such eventual self-destruction cannot be the stated objective of Nature, this unrelenting march toward collapse is restrained by the anti-world effects we have described earlier. Since the anti-world moderates the real, a reversed sequential direction effectively inhibits the drive towards self-destruction motivated by the simultaneous increase of λ and the increased noninjectivity of forward iterations, and the resulting state of dynamic equilibrium is the observed equilibrium of Nature. Like all others, nature's *kitchen* $C \times \mathfrak{C}$ where the actual dynamical processes occur is beyond direct observation; only its moderating effect in $C \times C$ is perceived by the observer in $\mathcal{D}(f) = C$.

As an example of this line of reasoning, consider an isolated system of two parts with each locally in equilibrium with its environment as in Eq. (18) that can now be re-expressed as

$$\widetilde{S_C}(t) = \widetilde{S_{C0}} + \left[N_A c_A \ln \left(\frac{T}{T_A(t)} \right) + N_B c_B \ln \left(\frac{T}{T_B(t)} \right) \right] -$$

$$- R \left[N_A \ln \left(\frac{P_A}{p_A(t)} \right) + N_B \ln \left(\frac{P_B}{p_B(t)} \right) \right], \quad (40)$$

where we note with reference to Fig. 3 that $T_A = T_1$, $T_B = T_2$ are the temperatures of subsystems A and B , $V_A + V_B = V$ is the total volume of C , p_A , p_B are the pressures of A and B , $P_{A,B} := N_{A,B}RT_{A,B}/V$ are their partial pressures with $P = P_A + P_B$ the total pressure exerted by the gases in V , and T is the equilibrium temperature of (20).

Then

(i) If the halves containing nonidentical ideal gases at different temperatures are brought in contact with each other, the equilibrium state of stasis resulting from the flow of *heat* and *cold* (= anti-heat) between the bodies lead to the equality of temperature, $T_A = T = T_B$, leading to the vanishing of the first part of Eq. (40).

(ii) If the gas in the first half expands into the second then equilibrium is reached when the *gas outflow* from the first half into the second is exactly balanced by the *vacuum inflow* from the second into the first if the second is evacuated, or if filled with a nonidentical gas then equalization of pressure of the chambers by outflow of the gases from their respective halves into the other, results in the vanishing of the second term of (40). In either of these cases competitive collaboration of the two halves, one with greater resources than the other, rather than annihilation of the weaker by the more resourceful leads to the state of mutual equilibrium.

In all these instances, the effect of the antiworld on the real is to moderate, inhibit or contain the consequence of the latter: this is its only manifestation in the observable real world. Thus *cold*, *vacuum* and *a nonidentical substance* are the negations of *heat* and *matter* — just as $-r \in \mathbb{R}_-$ is the negation of $r \in \mathbb{R}_+$. These negations as elements of the anti-world are no more observable than -5 , for example, is to us in our real world: we cannot have -5 objects around us, or measure the distance between two places to be -100 kilometers. Nonetheless, without \mathbb{R}_- there would be no zero, no starting initial point in any ordered set, and no “equilibrium” either. Nature, propelled by the unidirectional increase in entropic disorder, without the moderating influence induced by its anti-self, would have possibly crashed out of existence long ago!

In summary, then, for an interaction $f : C \rightarrow C$ and the bijective map $\mathfrak{f} : C \rightarrow \mathfrak{C}$ of Eq. (38b), the hierachal order

$$\begin{aligned} \text{Dynamics of } \mathfrak{f}f : C \rightarrow \mathfrak{C} \text{ in nature's } \textit{kitchen} (C, \mathcal{W}) \times (\mathfrak{C}, \mathcal{W}_\ominus) \\ \longrightarrow \text{Evolution of } f \text{ on } (C, \mathcal{W})^2 \\ \longrightarrow \text{Experimental observables in } \mathcal{D}(f) = C \end{aligned}$$

governed by

► Basic global irreversible unidirectional evolution of f driven by ininality of topology generated on C by the interaction f . The function-multiplication asymmetry between f and f^- is responsible for the unidirectionality of ininality,

► Induced local bi-directional dynamics of f in C^2 generated by the inhibitory influence of the anti-space $(\mathfrak{C}, \mathcal{W}_\ominus)$ on (C, \mathcal{W}) that moderates the global forward evolution in C^2 to a state of dynamical balance between the competitively collaborating interactions generated by f and f^- ,

define the state of equilibrated stasis schematized in Fig. 3. Recalling the discussion in connection with Fig. 1 that ininality is an effective expression of *non-bijective homeomorphicism* in which the sequence of evolutions (f^n) become progressively bijective, according to (6), on the saturated open sets of equivalence classes and their respective images, it can be argued that *the incentive towards the resulting effective simplicity of invertibility on the definite classes of sets*

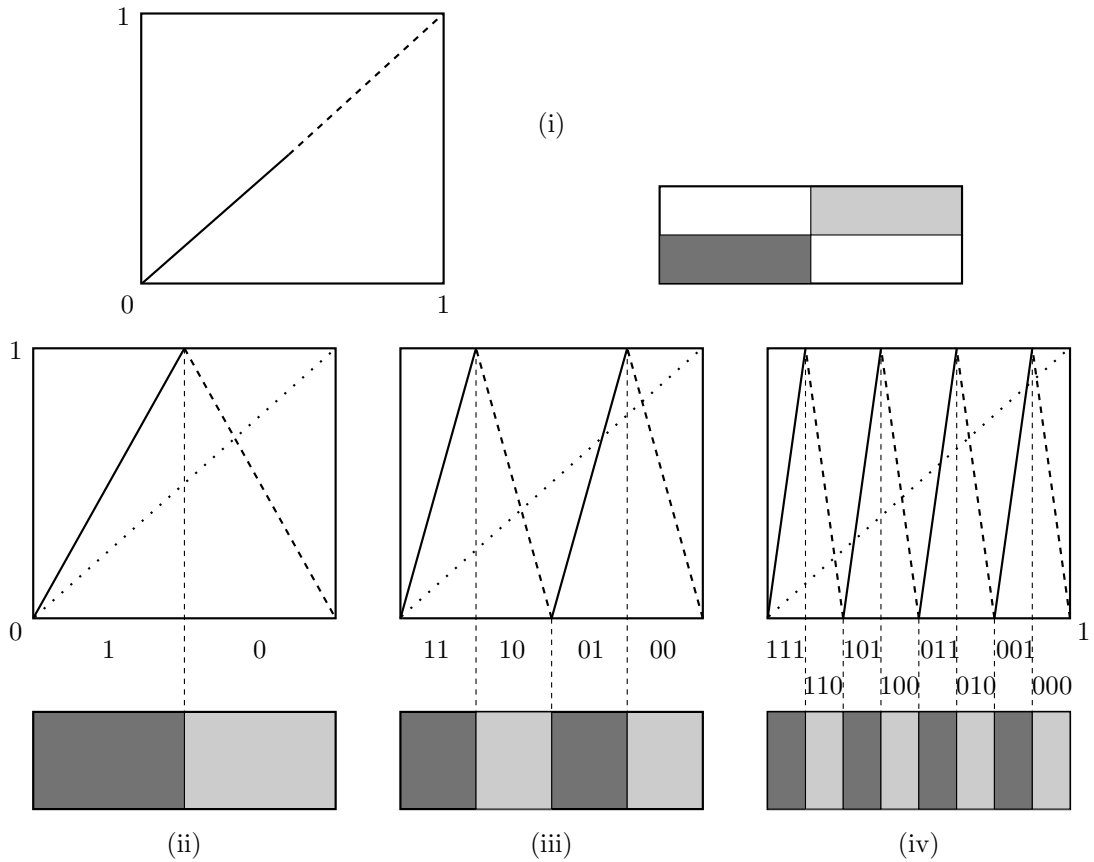


Figure 4: Matter-antimatter synthesis of an evolving system $C = A \cup B$ under the tent interaction. Here A is represented by the solid line while the dashed corresponds to the anti-set \mathfrak{B} . Taking $T_A > T_B$, $p_A > p_B$ and $\mu_A > \mu_B$, the dynamical evolution expressed by the shaded boxes would, in the absence of backward evolution induced by the anti-space, eventually be spread uniformly over the full domain, and equilibrium would be characterized solely by T_A , p_A , μ_A from the complete annihilation of B . The backward evolution from the exclusion topology of \mathfrak{B} leads to the equilibrated stasis shown. Denoting matter by 1 and (the effect of) anti-matter by 0, a progressively refined partition of $\mathcal{D}(t)$ generated by the evolving map is indicated in (ii), (iii) and (iv), where the partitioning sequence indicated is not that generated by the symbolic dynamics of the map. In the real world of the figure, matter-antimatter components are distinguished as injective branches with positive and negative slopes, and it is seen that their directional arrows oppose each other. And it is of course only this (increasing) non-injectivity that leads to the interesting competing collaborative dynamics of C .

associated with (f^n) is responsible for the evolutionary dynamics on C .

The present exposition of “providing a mechanical (i.e., dynamical) explanation of why classical systems behave thermodynamically” (Callender, 1999), is to be compared and contrasted with the approaches of Goldstein and Lebowitz (2004) and Callender (1999), see also Sklar (1993). The fundamental point of departure of our formulation lies in its non-subscription to the Newtonian paradigm of *microscopic* Hamilton’s equations yielding the Liouville equation for density distribution of *macroscopic* mechanical processes; as so eloquently espoused by Baranger (2000), can the emerging evolutionary properties of strongly nonlinear, self-organizing systems be successfully modelled by linear (Hamiltonian) differential equations (of motion)? By employing functional interactions as solutions to *difference equations* by the technique of graphical convergence of their iterates (in preference to linear differential equations), we explicitly involve the past in predicting the future and are thereby able to circumvent the issues of time reversal invariance and Poincaré recurrence that are inherently associated with the microscopic dynamics of Hamilton’s differential equations. This also enables us to avoid direct reference to statistical and probabilistic arguments except in so far as implied by the Axiom of Choice.

2.3 An Index of Nonlinearity: Complexity

With ininity in the cartesian space $C \times C$ serving as the engine for the increase of evolutionary entropic disorder, we now examine how a specifically nonlinear index can be ascribed to chaos, nonlinearity and complexity, and thereby to serve as the benchmark for chanoxity. For this, we first recall two non-calculus formulations of entropy that measure the complexity of dynamics of evolution of a map f .

Let $\mathcal{A} = \{A_i\}_{i=1}^I$ be a disjoint partition of non-empty subsets of a set X ; thus $\bigcup_{i=1}^I A_i = X$. The entropy

$$S(\mathcal{A}) = - \sum_{i=1}^I \mu(A_i) \ln(\mu(A_i)), \quad \sum_{i=1}^I \mu(A_i) = 1 \quad (41)$$

of the partition \mathcal{A} , with $\mu(A_i)$ some normalized invariant measure of the elements of the partition, quantifies the uncertainty of the outcome of an experiment on the occurrence of any element A_i of the partition \mathcal{A} . A refinement $\mathcal{B} = \{B_j\}_{j=1}^{J \geq I}$ of the partition \mathcal{A} is another partition such that every B_j is a subset of some $A_i \in \mathcal{A}$, and the largest common refinement

$$\mathcal{A} \bullet \mathcal{B} \stackrel{\text{def}}{=} \{C : C = A_i \cap B_j \text{ for some } A_i \in \mathcal{A}, \text{ and } B_j \in \mathcal{B}\}$$

of \mathcal{A} and \mathcal{B} is the partition whose elements are intersections of those of \mathcal{A} and \mathcal{B} . The entropy of $\mathcal{A} \bullet \mathcal{B}$ is given by

$$\begin{aligned} S(\mathcal{A} \bullet \mathcal{B}) &= S(\mathcal{A}) + S(\mathcal{B} | \mathcal{A}) \\ &= S(\mathcal{B}) + S(\mathcal{A} | \mathcal{B}), \end{aligned} \quad (42)$$

where the weighted average

$$S(\mathcal{B} | \mathcal{A}) = \sum_{i=1}^I P(A_i) S(\mathcal{B} | A_i) \quad (43a)$$

of the conditional entropy

$$S(\mathcal{B} \mid A_i) = - \sum_{j=1}^J P(B_j \mid A_i) \ln(P(B_j \mid A_i)) \quad (43b)$$

of \mathcal{B} given $A_i \in \mathcal{A}$, is a measure of the uncertainty of \mathcal{B} if at each trial it is known which among the events A_i has occurred, and

$$P(B_j \mid A_i) = \frac{P(B_j \cap A_i)}{P(A_i)} \quad (43c)$$

yields the probability measure $P(B_j \cap A_i)$ from the conditional probability $P(B_j \mid A_i)$ of B_j given A_i , with $P(A)$ the probability measure of event A .

The entropy (41) of the refinement \mathcal{A}^n , rather than (42), which has been used by Kolmogorov in the form

$$h_{\text{KS}}(f; \mu) \stackrel{\text{def}}{=} \sup_{\mathcal{A}_0} \left(\lim_{n \rightarrow \infty} \frac{1}{n} S(\mathcal{A}^n) \right) \quad (44)$$

to represent the complexity of the map as measuring the time rate of creation of information with evolution, yields $\ln 2$ for the tent transformation. Another measure the topological entropy $h_T(f) := \sup_{\mathcal{A}_0} \lim_{n \rightarrow \infty} (\ln N_n(\mathcal{A}_0)/n)$, where $N_n(\mathcal{A}_0)$ is the number of divisions of the partition \mathcal{A}^n derived from \mathcal{A}_0 that reduces to

$$h_T(f) = \lim_{n \rightarrow \infty} \frac{1}{n} \ln \mathcal{I}(f^n) \quad (45)$$

in terms of the number of injective branches $\mathcal{I}(f^n)$ of f^n for partitions generated by piecewise monotone functions, also yields $\ln 2$ for the entropy of the tent map. For the logistic map,

$$\mathcal{I}(f^n) = \mathcal{I}(f^{n-1}) + \langle \{x : x = f^{-(n-1)}(0.5)\} \rangle \quad (46)$$

yields the number of injective branches from the solutions of

$$\begin{aligned} 0 &= \frac{df^n(x)}{dx} = \frac{df(f^{n-1})}{df^{n-1}} \frac{df^{n-1}(x)}{dx} \\ &= \frac{df(f^{n-1})}{df^{n-1}} \frac{df(f^{n-2})}{df^{n-2}} \dots \frac{df(f)}{df} \frac{df(x)}{dx} \end{aligned}$$

that provide

$$x = \overbrace{f^{-}(\dots(f^{-}(f^{-}(0.5))) \dots)}^{(n-1) \text{ times}}, \quad n = 1, 2, \dots, (n-1);$$

here $\langle \{\dots\} \rangle$ is the cardinality of set $\{\dots\}$. It should be noted that in the context of the topological entropy, $\mathcal{I}(f)$ is merely a tool for generating a partition on $\mathcal{D}(f)$ by the iterates of f .

Examples. (1) In a fair-die experiment, if $\mathcal{A} = \{\text{even}, \text{odd}\}$ and the refinement $\mathcal{B} = \{j\}_{j=1}^6$ is the set of the six faces of the die, then for $i = 1, 2$

$$P(B_j \mid A_i) = \begin{cases} \frac{1}{3}, & j \in A_i \\ 0, & j \notin A_i, \end{cases}$$

and $S(\mathcal{B} \mid A_1) = \ln 3 = S(\mathcal{B} \mid A_2)$ according to Eq. (43b). Hence the conditional entropy of \mathcal{B} given \mathcal{A} , using $P(A_1) = 0.5 = P(A_2)$, is $S(\mathcal{B} \mid \mathcal{A}) = \ln 3$ by (43a), and

$$\begin{aligned} S(\mathcal{A} \bullet \mathcal{B}) &= S(\mathcal{A}) + S(\mathcal{B} \mid \mathcal{A}) \\ &= \ln 6, \end{aligned}$$

$$P(B_j \cap A_i) = \begin{cases} \frac{1}{6}, & j \in A_i \\ 0, & j \notin A_i. \end{cases}$$

If we have access only to partition \mathcal{B} and not to \mathcal{A} , then $S(\mathcal{B}) = \ln 6$ is the amount of information gained about the partition \mathcal{B} when we are told which face showed up in a rolling of the die; if on the other hand the only partition available is \mathcal{A} , then $S(\mathcal{A}) = \ln 2$ measures the information gained about \mathcal{A} on the knowledge of the appearance of an even or odd face.

(2) The dynamical evolution of Fig. 4 is a case in point of conditional probability and conditional entropy. Here the refinements of basic partition $\mathcal{A}_0 = \{\text{matter, antimatter}\} = \{A_{01}, A_{00}\}$ generated by the inverses of the tent map, interpreted as representing matter-antimatter dynamics, are denoted as $\mathcal{A}_n = \{t^{-n}(A_{0i})\}_{0,1}$ for $n = 1, 2, \dots$ to yield the largest common refinements

$$\mathcal{A}^n = \mathcal{A}_0 \bullet \mathcal{A}_1 \bullet \mathcal{A}_2 \bullet \dots \bullet \mathcal{A}_n, \quad n \in \mathbb{N}. \quad (47)$$

With reference to Fig. 4, these refinements are symbolically denoted by $\{1, 0\} \rightarrow \{11, 10, 01, 00\} \rightarrow \{111, 110, 101, 100, 011, 010, 001, 000\} \rightarrow \dots$, and $\mathcal{A}^n = \mathcal{A}_n$. Taking the measure of the elements of a partition to be its euclidean length, gives

$$P(A_{nj} \mid A_{0i}) = \begin{cases} \frac{1}{2^{n-1}}, & j \in A_{0i} \\ 0, & j \notin A_{0i}, \end{cases},$$

$S(\mathcal{A}_n \mid A_{0i}) = (n-1) \ln 2$, $i = 0, 1$, (Eq. 43b), $S(\mathcal{A}_n \mid A_0) = (n-1) \ln 2$, and finally $S(\mathcal{A}_n \bullet \mathcal{A}_0) = n \ln 2$. In case the initial partition \mathcal{A}_0 is taken to be the whole of $\mathcal{D}(t)$, then Eq. (41) gives directly $S(\mathcal{A}_n) = n \ln 2$.

(3) Logistic map $f_\lambda(x) = \lambda x(1-x)$, Nagashima and Baba (1999).

(i) $0 < \lambda \leq 3$, Fig. 5, can be subdivided into two categories. In the first, for $0 < \lambda < \lambda_1 = 2$, $\mathcal{I}(f_\lambda^n) = 2$ gives $h_T(f_\lambda) = 0$. This is illustrated in Fig. 5(a), (b), and (c) which show how the number of subsets generated on X by the increasing iterates of the map tend from 2 to 1 in the first case and to the set $\{\{0\}, (0, 1), \{1\}\}$ for the other two. The figure demonstrates that while in (a) the dynamics eventually collapses and dies out, the other two cases are equally uneventful in the sense that the converged multifunctional limits — of $(0, [0, 1/2]) \cup ((0, 1), 1/2) \cup (1, [0, 1/2])$ in figure (c), for example — are as much passive and displays no real “life”; this is quantified by the constancy of the lap number and the corresponding topological entropy $h_T(f) = 0$.

Although the oscillations in (d) for $\lambda = 3$ show more apparent “life” than the other cases, the iterates converge graphically to the tame $\{(0, [0, 2/3]) \cup ([0, 1], 2/3) \cup (1, [0, 2/3])\}$ indicated by the broken line and the topological entropy is again 0.

(ii) $3 < \lambda \leq 4$. As in (i), $h_T(f_\lambda) = 0$ whenever $\mathcal{I}(f_\lambda) \leq 2n$ which occurs, according to Fig. 6a, for $\lambda \leq \lambda_2 = 1 + \sqrt{5} = 3.23607$; here λ_n is the λ value at which a super-stable n -cycle appears. The super-stable λ for which $x = 0.5$ is fixed with respect to f^n , $n = 2^m$, $m = 0, 1, 2, \dots$, are of special significance as this is the only point in X at which f is injective; this leads to a simplification of the dynamics of the map that can be verified by comparing the plots in Figs. 5, 6a, and 6b. These super-cycles possess the great simplifying property that the stable

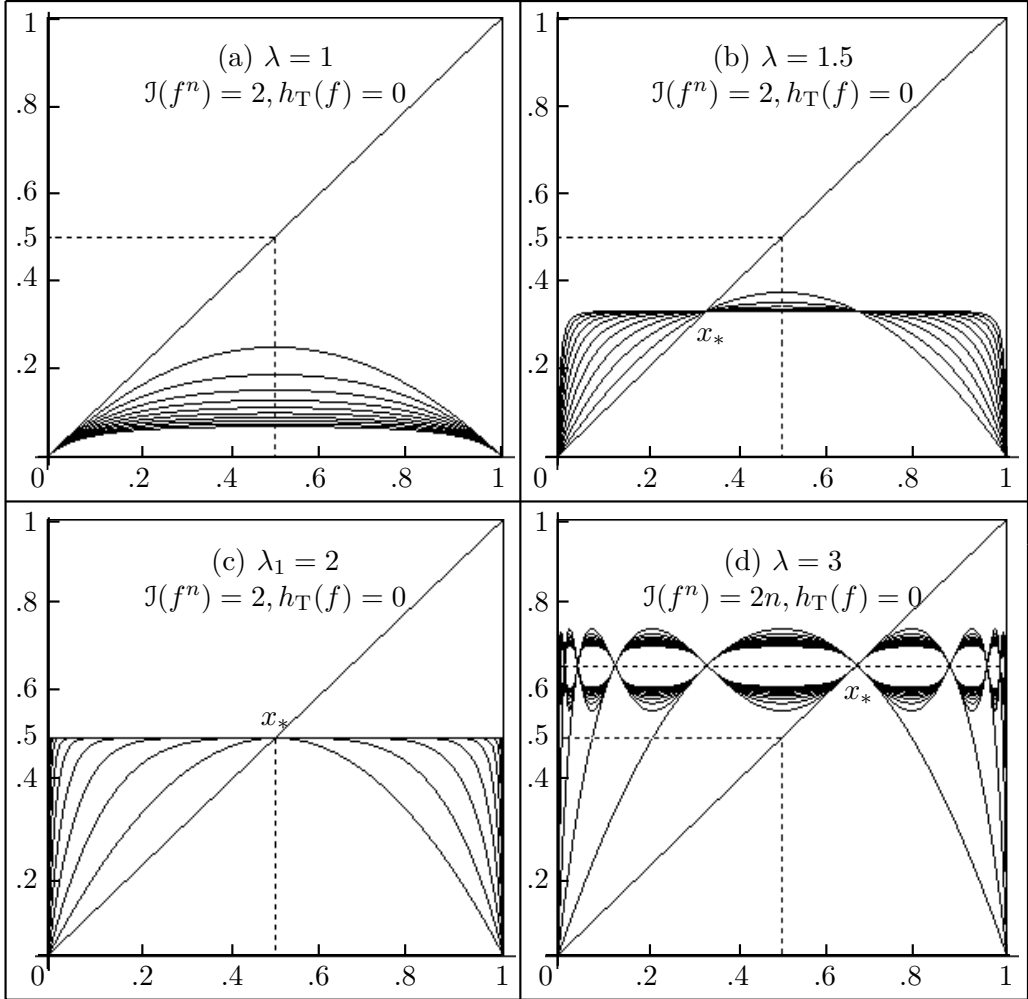


Figure 5: Non-life dynamics of the first 10 iterates of the logistic map $f_\lambda = \lambda x(1-x)$ generated by its only stable fixed point $x_* = (\lambda - 1)/\lambda$. Although the partition induced on $X = [0, 1]$ by the evolving map in (d) is refined with time, the *stability of the fixed point* $x_* = 0.6429$ prevents the dynamics from acquiring any meaningful evolutionary significance with the multifunctional graphical limit, indicated by the broken line, being of the same type as in (b) and (c): as will be evident in the following, *instability of the fixed point is necessary for the evolution of a meaningful complex life*. $\lambda_1 = 2$ of (c) — obtained by solving the equation $f_\lambda(0.5) = 0.5$ — is special because its super-stable fixed point $x = 0.5$ is the only point in $\mathcal{D}(f)$ at which f is injective and therefore well-posed by this criterion.

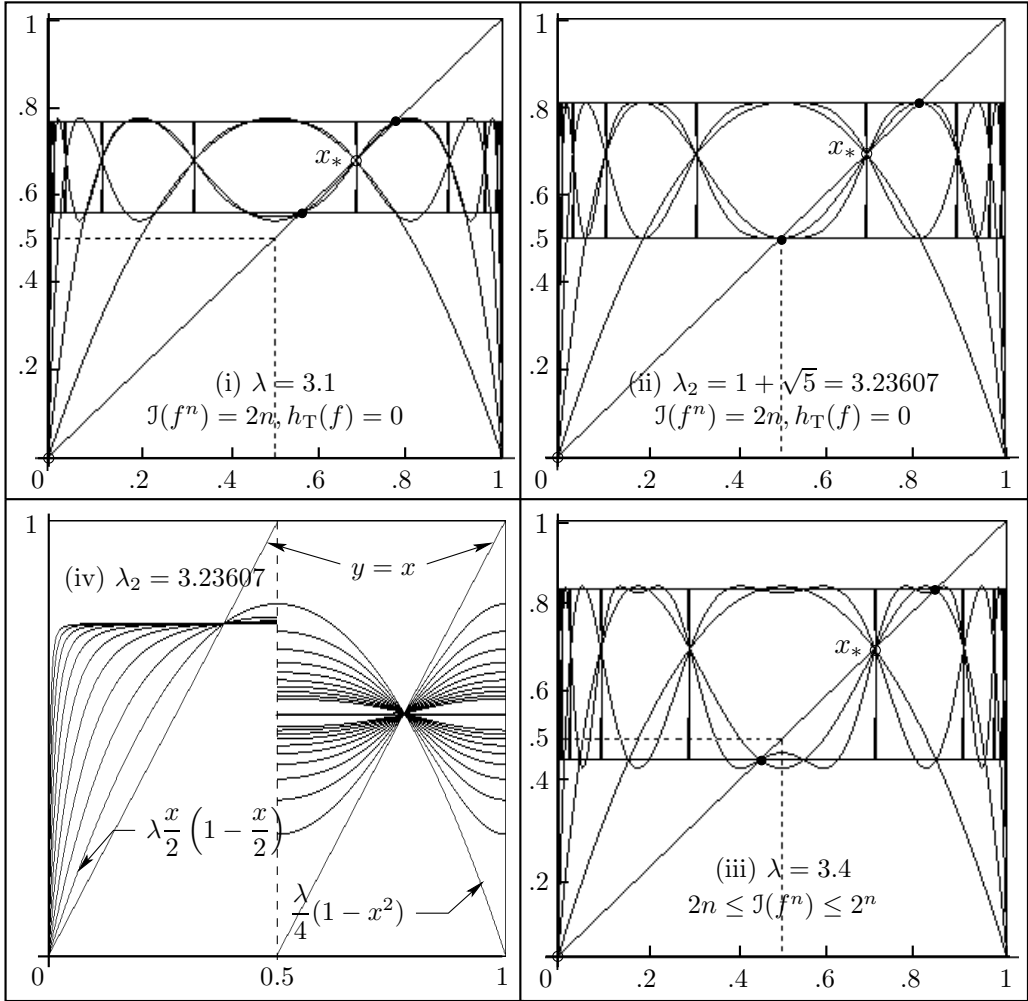


Figure 6a: Dynamics of stable 2-cycle of the logistic map, where each panel displays the first four iterates superposed on the graphically converged multifunction represented by iterates 1001 and 1002. The unstable fixed point x_* of f is directly linked to its stable partners a and b of f^2 that report back to their master x_* . Compared to case (i) where the relative simplicity of the instability of x_* allows its stable partners to behave monotonically as in Fig. 5(b), in (iii) the instability is strong enough to induce the oscillatory mode of convergence of Fig. 5(iv). Case (ii) of the super-stable cycle for $\lambda_2 = 1 + \sqrt{5}$ — obtained by solving the equation $f_\lambda^2(0.5) = 0.5$ — reflecting well-posedness of f at $x = 0.5$ represents, as in Fig 5(iii), a mean of the relative simplicity of (a) and the complex instability of (iii) that grows with increasing λ due to the fact that $\lambda > \lambda_2$ ensures $f_\lambda^2(0.5) = f_\lambda(\lambda/4) < 0.5$. Notice that in all the three cases, $\langle \{x : f_\lambda^n(x) = 0.5\} \rangle = 2$ for all n . Panel (iv), in this and the following two subdiagrams, illustrates how the individual parts, acting independently on their own in the reductionist framework not in competitive collaboration, leads to an entirely different simple, non-complex, dynamics.

horizontal parts of the graphically converged multifunction are actually tangential to all the turning points of every iterate of f . The immediate consequence of this is that for a given $3 < \lambda < \lambda_* = 3.5699456$, with λ_* the value at the “edge of chaos”, the dynamics of f attains a state of basic evolutionary stability after only the first $\{2^m\}_{m \in \mathbb{N}}$ time steps in the sense that no new spatial structures *emerge* after this period, any further temporal evolution being fully utilized in spatially *self-organizing* this basic structure throughout the system by the generation of equivalence classes of the initial 2^m time steps.

When $\lambda > \lambda_2$ as in Figs. 6a and 6b the number of injective branches satisfy $2n \leq \mathcal{I}(f_\lambda^n) \leq 2^n$ and it is easily appreciated, from Eq. (46), the difficulty in actually calculating these numbers for large n . For $\lambda = 4$, however $\mathcal{I}(f_4^n) = 2^n$ and the topological entropy reduces to the simple $h(f_4) = \ln 2$; $h_T(f) > 0$ is sufficient condition for f_λ to be chaotic. The tent map behaves similarly and has an identical topological entropy, see Fig. 7a.

The difficulty in evaluating $\mathcal{I}(f^n)$ for large values of n and the open question of the utility of the number of injective branches of a map in actually measuring the complex dynamics of the nonlinear evolution of the logistic map suggests the significance of the role of *evolution of the graphs of the iterates of f_λ* in defining the nonlinear dynamics of natural processes. It is also implied that the dynamics can be simulated through *the partitions induced on $\mathcal{D}(f)$ by the evolving map* as described by graphical convergence of the functions in accordance with our philosophy that the dynamics on C derives from the evolution of f in C^2 as observed in $\mathcal{D}(f)$. The following subsection carries out this line of reasoning, to be compared with that embodied in Eqs. (44) and (45), to define a new index of chaos, nonlinearity and complexity, that of *chanoxity*.

2.3.1 ChaNoXity: A Measure of Chaos, Nonlinearity and Complexity

The blown-up view of the *stable* 8-cycle, Fig. 6c, of the logistic map graphically illustrates evolutionary dynamics arising from this interaction. The 2^3 *unstable* fixed points marked by open circles interact among themselves as implied in the figure to generate the stable periodic cycle, providing thereby a vivid illustration of competitive collaboration between world-antiworld effects. The *self-organized collaboration* is due to the emergent irreversible urge toward bijective simplicity of ininity accompanying increasing λ as manifest in the Second Law increase of entropy; this is inhibited locally for a fixed λ by an opposing *competitive anti-effect* that eventually leads to the stable periodic orbit. This local inhibitory restraining effect appears in the figure as the opposing change of slope associated with each of the unstable fixed points except the first at $x = 0$ which must now be paired with its equivalent image at $x = 1$. Display (c) of the partially superimposed limit graphs 1001-1008 — that remain invariant with further temporal evolution — on the first 8 iterates illustrate that while nothing new emerges beyond this initial period, *further temporal evolution propagates the associated changes throughout the system as self-generated equivalence classes acting as inhibitors that restrain the system to a state of local* (that is spatial, for the given λ) *periodic stasis*. As compared to Fig. 4 for the tent interaction, this manifestation of antieffects in the logistic for $\lambda < \lambda_* = 3.5699456$ has a profound feature that deserves attention: while in the former the antimatter branch belongs to distinct fixed points of equivalence classes, in the later matter-antimatter competitive-collaboration is associated with each of the 2^N generating fixed point branches possessing bi-directional characteristics with the inhibition of antimatter actually generating the equivalence class. In the observable real world of $\mathcal{D}(f)$, this has the interesting consequence that whereas the tent interaction generates matter-antimatter intermingling of disjoint components to produce the homogenization of Fig. 4, for the logistic the resulting behaviour is a consequence of a deeper interplay of

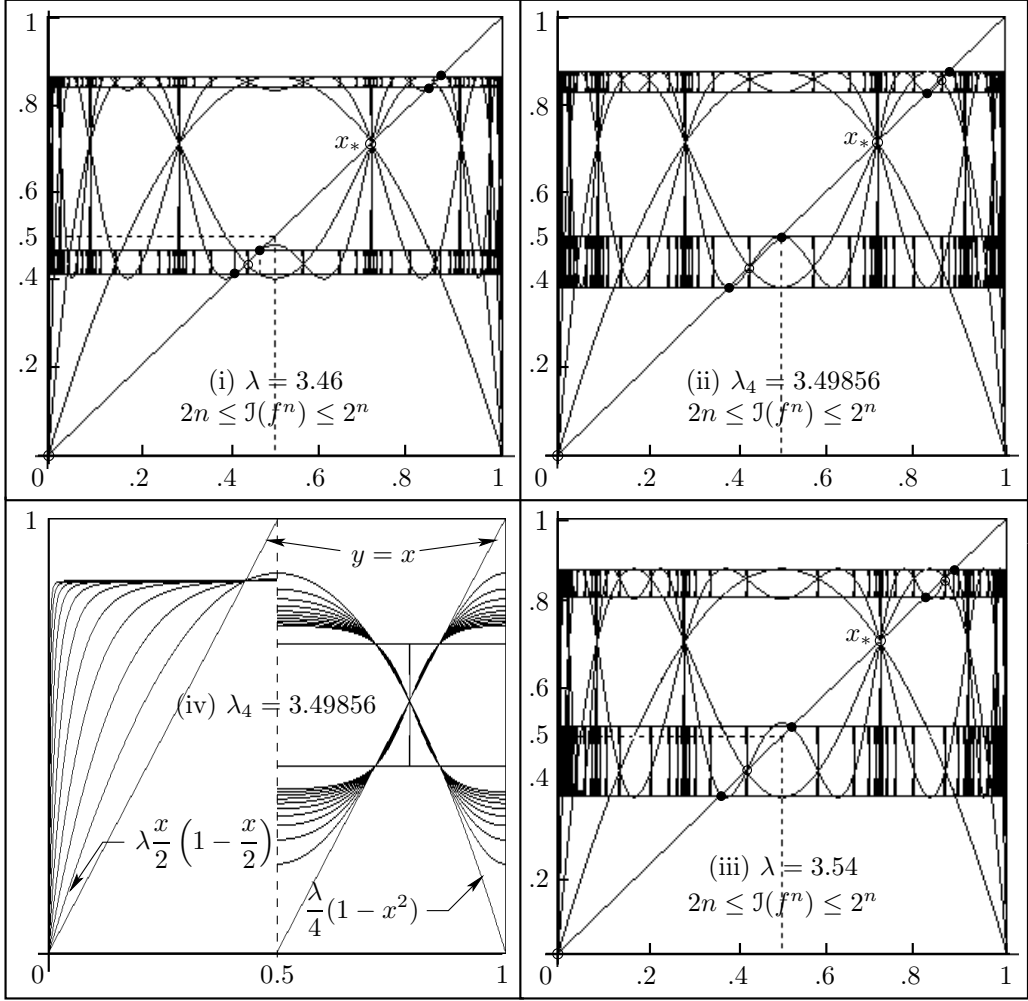


Figure 6b: Dynamics of stable 4-cycle of the logistic map, where each panel displays the first four iterates superposed on the graphically “converged” multifunction represented by iterates 1001-1004. The unstable basic fixed point x_* due to f is now linked to its *unstable* partners $\{a\}$ and $\{b\}$ denoted by open circles arising from f^2 , who report back to the overall controller x_* the information they receive from their respective stable committees $\{c, e\}$ and $\{d, f\}$. Compared to the 2-cycle of Fig. 6a, the instability of principal x_* is now serious enough to require sharing of the responsibility by $\{a\}$ and $\{b\}$ who are further constrained to delegate authority to the subcommittees mentioned above. Case (ii) of the super-stable cycle for $\lambda_4 = 3.49856$ — obtained by solving $f_\lambda^4(0.5) = 0.5$ — reflecting well-posedness of f at $x = 0.5$ represents as before the mean of the relative simplicity of (i) and the large instability of (iii).

the opposing forces leading to a higher level of complexity than can be achieved by the tent interaction. This distinction reflects in the interaction pair (f, \mathfrak{f}) that can be represented as

$$x \mapsto 2x \xrightarrow{\text{tent}} \begin{cases} 2x, & \text{if } 0 \leq x < 0.5 \\ 2(1-x), & \text{if } 0.5 \leq x \leq 1 \end{cases}, \quad x \mapsto 2x \xrightarrow{\text{logistic}} 4x(1-x), \quad (48)$$

which leads to the

Definition. Complex System, Complexity. The couple $((X, \mathcal{U}), f)$ of a topological space (X, \mathcal{U}) and an interaction f on it is a *complex system* if

(CS1) The *algebraic structure* of X consists of a family of progressively refined disjoint partitions of non-empty subsets induced by the iterates of f . Of these, only a *coarsest finite number determines the character of the system*, with successive refinements erecting on this defining foundation the structure of the system.

(CS2) The *topology* \mathcal{U} of X is generated *through a process of competitive collaboration among the hierarchy of partitions* in the sense that the subbasis of \mathcal{U} at any level of refinement is the union of the open sets of its immediate coarser partition and that generated independently by the partition under consideration; here all open sets are the saturated sets of equivalence classes under the iterates of the interaction.

The *complexity* of a system is a measure of the interaction between the different levels of partitions that are generated on $\mathcal{D}(f)$ under the induced topology on X .

Thus for example in Fig. 6a(ii) of the stable 2-cycle, the defining character is established by just the first 2 time steps which is then propagated throughout the system by the increasing ill-posedness of the future iterates, thereby establishing the global structure as seen in the diagram. The open sets of $\mathcal{D}(f)$ are the projections of the boxes onto the x -axis, with their boundary being represented by the members of the equivalence class $[x_*]$ of the unstable fixed point x_* . With increasing λ the complexity of the dynamics increases as revealed by the succeeding plots of 4- and 8-cycles; this allows us to define the *chanoxity index* of the interaction to be the constant ν that satisfies

$$f(x) = x^{1-\nu}, \quad \forall x \in \mathcal{D}(f). \quad (49a)$$

If $\langle f(x) \rangle$ and $\langle x \rangle$ are the measures that make Eq. (49a) possible, then in

$$\nu \stackrel{\text{def}}{=} 1 - \frac{\ln \langle f(x) \rangle}{\ln \langle x \rangle} \quad (49b)$$

we adopt the criteria that

(a) $\langle x \rangle$ is the number of basic unstable fixed points of f for any λ that is responsible for *emergence*. Thus for $1 < \lambda \leq 3$ there is just one unstable fixed point at $x = 0$, which is then followed by the familiar sequence of 2^N fixed points until $\lambda = \lambda_*$ when this number is infinite.

(b) For $f(x)$ the estimate

$$\langle f(x) \rangle = 2f_1 + \sum_{j=1}^N \sum_{i=1}^{2^{N-j}} f_{i,2^{N-j}}, \quad N = 1, 2, \dots,$$

where $f_i = f^i(0.5)$ and $f_{i,j} = |f^i(0.5) - f^j(0.5)|$, leads to the measure of the chanoxity index which for understandable reasons we call the dimensional chanoxity of $f_{\{\lambda\}}$.

$$\nu_N = 1 - \frac{1}{N \ln 2} \ln \left[2f_1 + \sum_{j=1}^N \sum_{i=1}^{2^{N-j}} f_{i,2^{N-j}} \right], \quad (50)$$

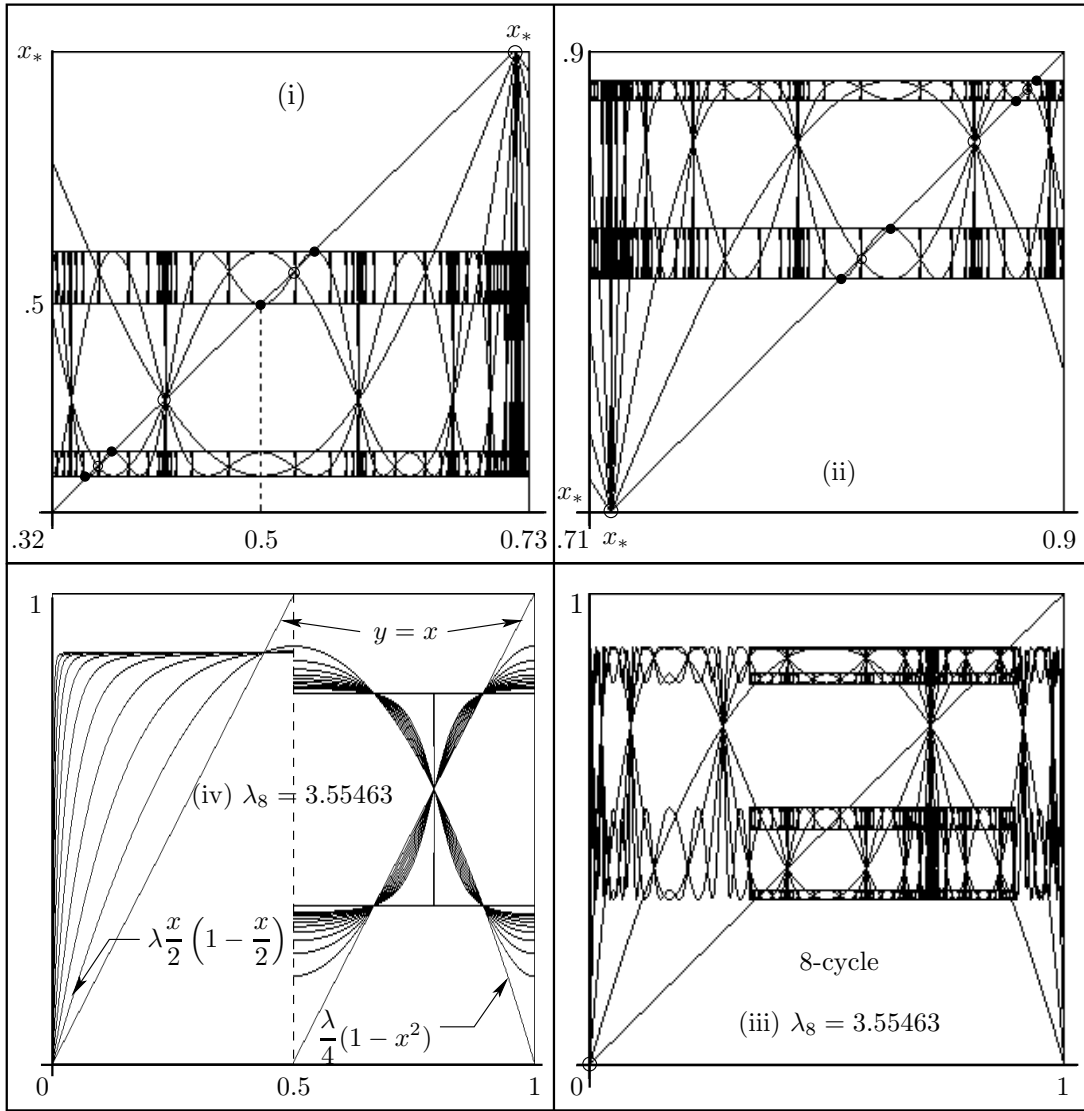


Figure 6c: Blown-up view of the *stable* 8-cycle graphically illustrates evolutionary dynamics arising from the logistic interaction. The 2^3 *unstable* fixed points marked by open circles interact among themselves as indicated to generate the stable periodic cycle providing thereby a vivid demonstration of competitive collaboration between world-antiworld effects. Display (iii) of the partially superimposed limit graphs 1001-1008 — that remain invariant with further temporal evolution — demonstrates that while nothing new emerges after the first 8 time steps, further evolution consolidates the associated changes throughout the system in the form of self-generated equivalence classes that act as the inhibitors toward a state of eventual stasis.

which which for understandable reasons we call the *dimensional chanoxity* of f_λ . for understandable reasons we call the *dimensional chanoxity* of f_λ .⁹ In the calculations reported here, λ is taken to correspond to the respective superstable periodic cycle, where we note from Figs. 5, 6a and 6b that the corresponding super-stable dynamics faithfully reproduces all the features of emergence and self organization of that stable 2^N cycle class.

λ	N	$f^{2N}(0.5)$	$\langle f(0.5) \rangle$	ν_N
2.0000000	—	0.50000	1.000000	0.000000
3.2360680	1	0.50000	1.927051	0.053605
3.4985600	2	0.50000	2.404122	0.367245
3.5546300	3	0.50001	2.680845	0.525771
3.5666700	4	0.50000	2.842181	0.623250
3.5692401	5	0.50001	2.935103	0.689318
3.5697999	6	0.50004	2.989741	0.736663
3.5699124	7	0.50001	3.019392	0.772249
3.5699439	8	0.50014	3.043283	0.799296
3.5699446	9	0.49994	3.050981	0.821192
3.5699451	10	0.50016	3.059756	0.838658
↓	↓	⋮	↓	↓?
3.5699456	∞	—	3.??????	1.000000

Table 5a: In the passage to full chaoticity, the system becomes increasingly complex and nonlinear (remember: chaos is maximal nonlinearity) such that at the edge of chaos $\lambda = \lambda_* = 3.5699456$, the system is completely complex and chaotic with $\nu = 1$. For $1 < \lambda \leq 3$ with no generated instability of which $\lambda = 2$ is representative, $\nu = 1 - \ln(1/2 + 1/2)/\ln 1$.

The numerical results of Table 5a suggest that

$$\lim_{N \rightarrow \infty} \nu_N = 1$$

at the “edge of chaos” $\lambda = \lambda_* = 3.5699456$. Since $\nu = 0$ gives the simplest linear relation for f , values of 1 and $-\infty$ for the index indicate the largest non-linearity and complexity so that the logistic interaction is maximally complex at the transition to the fully chaotic region. For this range of values $3 \leq \lambda \leq \lambda_*$, the associated increasing energy input to the system is fully utilized in enhancing its complexity through increasing structural emergence with the accompanying self-organization transmitting this emerging behaviour throughout the system as enumerated earlier.

What happens for $\lambda > \lambda_*$ in the fully chaotic region where emergence persists for all times $N \rightarrow \infty$ with no self-organization, is shown in Table 5b which indicates that on crosssing the chaotic edge, the system abruptly transforms to a state of *effective linear simplicity* that can

⁹Recall that the fractal dimension of an object is formally defined very similarly:

$$D = \frac{\ln(\# \text{ self-similar pieces into which the object can be decomposed})}{\ln(\text{magnification factor that restores each piece to the original})}.$$

λ cline3-9		N						→	∞
		12	14	16	18	20			
3.57	$\langle f(0.5) \rangle$	4.387099	6.626634	13.76167	40.47870	145.5237	?	0.0000	
	ν_N	0.822228	0.780513	0.763589	0.703384	0.640744			
3.6	$\langle f(0.5) \rangle$	290.3677	1171.071	4555.594	17900.68	73980.36	?	0.0000	
	ν_N	0.318189	0.271885	0.241411	0.215127	0.191258			
3.7	$\langle f(0.5) \rangle$	950.8090	3828.215	14796.66	61351.94	236962.9	?	0.0000	
	ν_N	0.175582	0.149825	0.134188	0.116399	0.107285			
3.8	$\langle f(0.5) \rangle$	1162.450	4612.551	18565.80	74061.57	295511.7	?	0.0000	
	ν_N	0.151421	0.130618	0.113728	0.101309	0.091357			
3.9	$\langle f(0.5) \rangle$	1390.724	5703.793	22384.97	90580.02	359594.0	?	0.0000	
	ν_N	0.129865	0.108735	0.096860	0.085172	0.077200			
↓	⋮	↓?	↓?	↓?	↓?	↓?	↙?		
4.0	ν_N	0.0000	0.0000	0.0000	0.0000	0.0000		0.0000	

Table 5b: Illustrates how the fully chaotic region of $\lambda_* < \lambda \leq 4$ is effectively “linear” with self-organization and emergence implying each other. The jump discontinuity in ν at the edge of chaos λ_* reflects a qualitative change in the dynamics, with all the gainfully employed energy input for $\lambda \leq \lambda_*$ employed in the generation of the complex internal structures of the system being fully utilized in generating the emerging characteristics without any self-organization as $\lambda \rightarrow 4$.

be interpreted to result from the drive toward ininality and effective bijectivity on saturated sets and on the image component space of f . This jump discontinuity in ν demarcates order from chaos, linearity from (extreme) nonlinearity, and simplicity from complexity. This non-organizing region $\lambda > \lambda_*$ of deceptive non-life simplicity characterized by dissipation and irreversible “frictional losses”, is to be compared and contrasted with the nonlinearly complex region $3 < \lambda \leq \lambda_*$ where irreversibility generates self-organizing, useful changes in the internal structure of the system in order to attain the levels of complexity needed in the evolutionary process. While the state of eventual evolutionary stasis appears in $3 < \lambda \leq \lambda_*$, the relative linear simplicity of $\lambda > \lambda_*$ arising from the competitive dissipatory losses characteristic of this region conceals the resulting self-organizing thrust on $3 < \lambda \leq \lambda_*$ of the higher periodic windows of this region, with the smallest period 3 appearing at $\lambda = 1 + \sqrt{8} = 3.828427$. By the Sarkovskii ordering of natural numbers, there is embedded in this fully chaotic region a backward directional arrow that induces a return to lower periodic stability that eventually terminates with the period doubling sequence in $3 < \lambda \leq \lambda_*$. This spatial λ -induced global dissipative decrease in λ in the face of the prevalent increase towards $\lambda > \lambda_*$ that can be taken to be a result of the anti-world effects, is schematically summarized in Fig. 7a and is expressible as

$$x \xrightarrow{\text{logistic}} f_\lambda(x) \left\{ \begin{array}{l} 3 < \lambda \leq \lambda_*, 0 < \nu \leq 1, \text{ self-organizing complex system} \\ \xrightarrow{\text{inality}} \lambda_* < \lambda \leq 4, \nu = 0, \text{ dissipative complex system} \end{array} \right\} \begin{array}{l} \xleftarrow{\text{(Sarkovskii)}} \\ \xrightarrow{\text{effects}} \end{array} \quad (51)$$

Under normal circumstances dynamical equilibrium is attained, as elaborated earlier, within the local *temporal* (that is with respect to the iterates) self-organizing component of the loop above.

If however the system is *spatially* driven (by an increasing λ) into the dissipative region, the global latent anti-world effects of its periodic stable windows acts as a deterrent and, prompted by the Sarkovskii ordering, induces the system back to the self-organizing region of equilibration. This condition of dynamical stasis is thus marked by a balance of *both the spatial and temporal effects*, with each interacting synergetically with the other to generate an optimum dynamical state of stability. Reference to Figs. 6a, 6b and 6c clearly illustrates that new, distinguishing and non-trivial features of the evolutionary dynamics occur at the 2^N unstable fixed points of f_λ leading to the *emerging* patterns that clearly characterize the resources λ available to the interaction. These figures also illustrate the *self-organization* induced by further passage of time by distributing this emergent pattern throughout X in the form of equivalence classes of these 2^N basic fixed points. Panel (a) of Fig. 7a magnifies these features of the defining fixed points and their classes for $\lambda < \lambda_*$ to generate the stable-unstable signature in the graphically convergent limit of $t \rightarrow \infty$, essentially reflecting the competitive cohabitation of the matter-antimatter components associated with these points. This in turn introduces a sense of symmetry with respect to the input-output axes of the interaction that, as shown in panel (c), is broken when $\lambda > \lambda_*$ with the boundary of the “edge of chaos” signalling this physical disruption with a discontinuity in the value of the chanoxy index ν .

Figure 7a(d) which summarizes these observations, identifies the self-organizing emergent region $3 < \lambda \leq \lambda_*$ as the life generating and sustaining complex domain (B) of the logistic interaction f_λ . Below a value of 3, the resources of f_λ are insufficient for supporting life while above 3.5699456, too much “heat” is produced for sustenance of constructive competition between the opposing directions, with the forward drive toward uniformity of ininality effectively destroying the containing reverse competition. By contrast, Fig. 7b confirms 6a, 6b and 6c that independent reductionist behaviour of the components of a system cannot generate chaos or complexity.

3 Conclusions: The Mechanics of Thermodynamics

In this paper we have presented a new approach to the nonlinear dynamics of evolutionary processes based on the mathematical framework and structure of multifunctional graphical convergence introduced in Sengupta (2003). The basic point we make here is that the *macroscopic* dynamics of evolutionary systems is in general governed by strongly nonlinear, non-differential laws rather than by the Newtonian Hamilton’s linear differential equations of motion

$$\frac{d\mathbf{x}_i}{dt} = \frac{\partial H(\mathbf{x})}{\partial \mathbf{p}_i}, \quad \frac{d\mathbf{p}_i}{dt} = -\frac{\partial H(\mathbf{x})}{\partial \mathbf{x}_i}, \quad -\infty < t < \infty \quad (52)$$

for the position $\mathbf{x}_i(t)$ and momentum $\mathbf{p}_i(t)$ of the N particles of an isolated (classical) system in its phase space of microstates $\mathbf{x}(t) = (\mathbf{x}_i(t), \mathbf{p}_i(t))_{i=1}^N$, translated to Liouville Equation for the macroscopic system. As is well known, Hamiltonian dynamics leads directly to the microscopic-macroscopic paradoxes of Loschmidt’s time-reversal invariance of Eq. (52) according to which all forward processes of mechanical system evolving according to this law must necessarily allow a time-reversal that would require, for example, that the Boltzmann H -function decreases with time just as it increases, and Zarmelo’s Poincare recurrence paradox which postulates that almost all initial states of isolated bounded mechanical system must recur in future, as closely as desired. One approach — Goldstein and Lebowitz (2004), Price (2004) — to the resolution of these paradoxes entail

(1) A “fantastically enlarged” phase space volume as the motivating entropy increasing force. Thus, for example, a gas in one half of a box equilibrates on the whole on removal of the

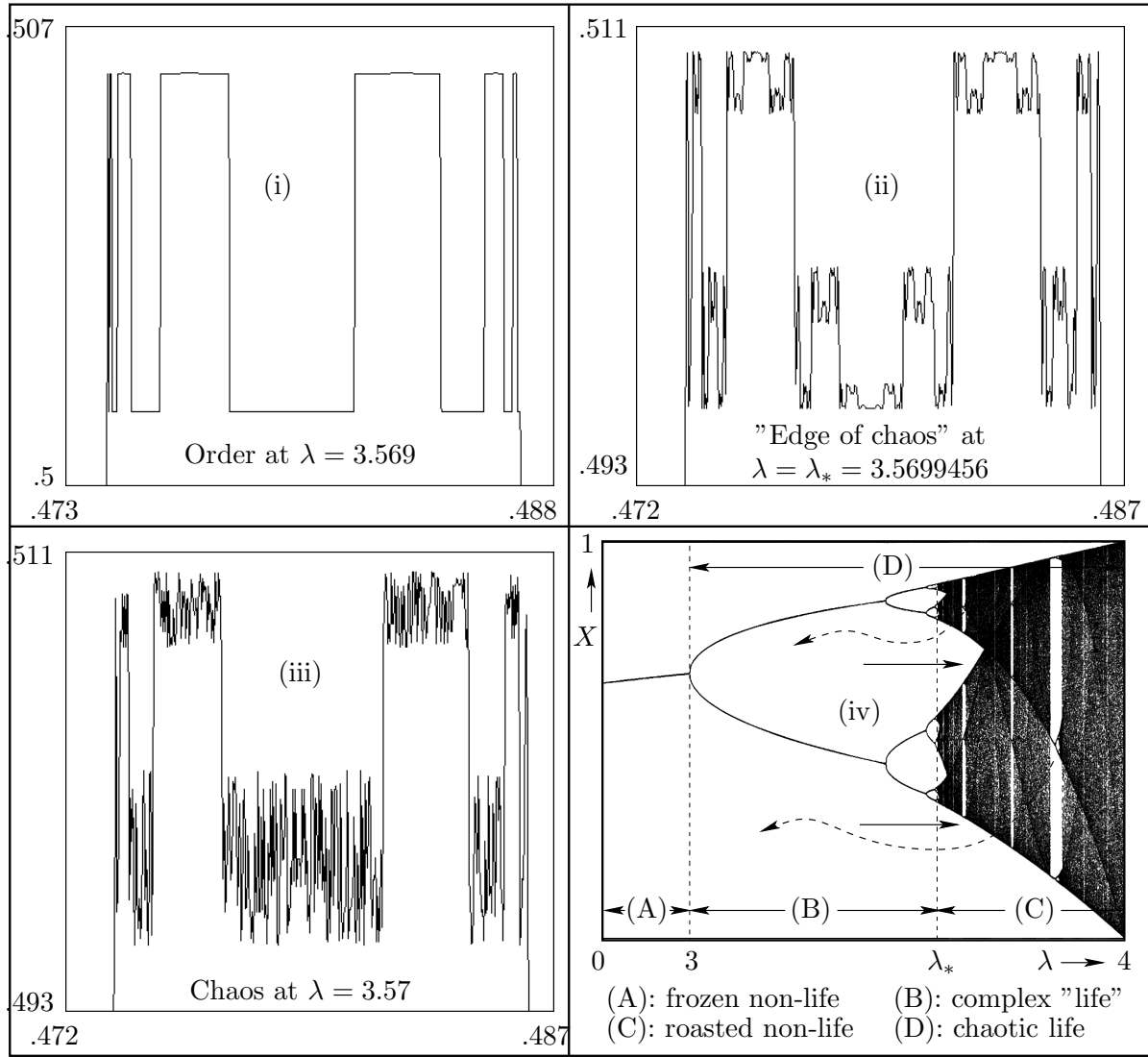


Figure 7a: In contrast with the relatively tame (i) and (ii), panel (iii) illustrates the property of fully chaotic maximal ill-posedness and instability. Here $\mathcal{I}(f^n) = 2^n$, and the topological entropy $h_T(f) = \lim_{n \rightarrow \infty} \ln(\mathcal{I}(f^n))/n = \ln 2$. In (iv) we illustrate the evolution of natural processes under the logistic interaction as summarized in panels (i)–(iii) and in Eq. (51). The dashed arrows indicate Sarkovskii stabilization of the full-arrowed, entropic, initial drive towards a state of superheated, chaotic, non-life illusory simplicity when the non-trivial fixed point no longer determines the fate of the evolutionary dynamics of the system, thereby establishing a *chaotically complex* state of dynamical equilibrium. A typical example of life-defining complex system (B) is the parliamentary system of governance with the speaker of the House acting as the supreme non-trivial fixed authority of the constitutional interaction between the ruling party and the opposition, while the Iraq war and its aftermath offers a versatile model of chaotic complexity (D).

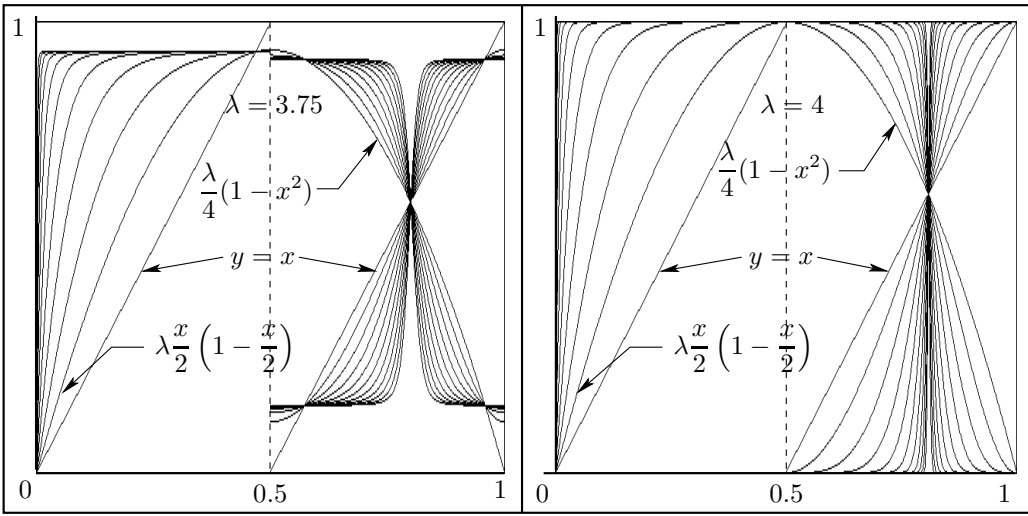


Figure 7b: Reductionism cannot generate chaos or complexity. Together with Figs. 6a, b, and c, the present figure and this display clearly illustrates the unique role of non-injective ill-posedness in defining chaos and complexity. Although on its own, $\lambda(1 - x^2)/4$ can generate by splitting its unsteady self into two steady state products, this “asexual” production of “life” is not nearly structurally as rich and varied as its “sexual” counterpart. A consequence of this is that unlike in its bidirectional complex logistic mode, the unidirectional component *does not generate any qualitative changes in the character of its evolutionary dynamics with a change in the value of λ .*

partition so as to reach a state in which the phase space volume is almost as large as the total phase space available to the system under the imposed constraints, when the number of particles in the two halves essentially become equal. In this situation, Boltzmann identifies, *for a dilute gas* of N particles in a container of volume V under weak two-body repulsive forces satisfying essentially the linearity condition $V/N \gg b^3$ with b the range of the force, the thermodynamic entropy of Clausius with $S_B = k \ln |\Gamma(M)|$, where $\Gamma(M)$ is the region in $6N$ -dimensional Liouville phase space of the microstates belonging to the equilibrium macrostate M in question. When the system is not in equilibrium, however, the phase space arguments imply that the relative volume of the set of microstates corresponding to a given macrostate for which evolution leads to a macroscopic decrease in the Boltzmann entropy *typically* goes exponentially to zero as the number of atoms in the system increases. Hence for a macroscopic system “the fraction of microstates for which the evolution leads to macrostates with larger Boltzmann entropy is so close to one that such behaviour is exactly what should be seen to always happen”, Lebowitz (1999).

(2) The statistical techniques implicit in the foregoing interpretation of *macroscopic irreversibility in the context of microscopic reversibility of Newtonian mechanics* rely fundamentally on the conservation of Liouville measures of sets in phase space under evolution. This means that if a state $M(t)$ evolves as $M(t_1) \stackrel{t_1 \leq t_2}{\equiv} M(t_2)$ such that the evolved phase space $\Gamma_{t_2}(M(t_1))$ of $M(t_1)$ is necessarily contained in $\Gamma(M(t_2))$ by the arguments in (1), then the preservation of measures requires that $\Gamma_{t_2}(M(t_1)) \leq \Gamma(M(t_2))$, thereby verifying the increase of S_B . Identifying the macrostate of a system with our interaction image $f(x)$ of a microstate x in “phase space” $\mathcal{D}(f)$ that generates the equivalence class $[x]$ of microstates, invariance of phase space volume can be interpreted to be a direct consequence of the *linearity assumption of the Boltzmann interaction for dilute gases* that is also inherent in his *stosszahlansatz* assumption of molecular chaos that neglects all correlations between the particles.

(3) Various other arguments like cosmological big bang and the relevance of initial conditions preferring the forward direction to the reverse are invoked to argue a justification for macroscopic irreversibility, that in the ultimate analysis is a “consequence of the great disparity between microscopic and macroscopic scales, together with the fact (or very reasonable assumption) that what we observe in nature is typical behaviour, corresponding to typical initial conditions”, Goldstein and Lebowitz (2004).

In comparison the multifunctional graphical convergence techniques, founded on difference rather than differential equations, adapted here avoids much of the paradoxical problems of calculus-based Hamiltonian mechanics, and suggests an alternate specifically nonlinear dynamical framework for the dissipative dynamical evolution of Nature that support self-organization, adaption, and emergence in complex systems. The significant contribution of the difference equations is that evolution at any time depends explicitly on its immediate predecessor — and thereby on all its predecessors — leading to non-reductionism, self-emergence, and complexity.

Acknowledgements. It is my pleasure and privilege to acknowledge a deep sense of gratitude to the participants of the international workshop *Mathematics and Physics of Complex and Nonlinear Systems* that was held at IIT Kanpur, March 14-26 2004, for having elevated the proceedings to great heights through their dedicated multiple lectures and the consequent discussions during this 2-week period. The present paper has benefitted immensely from the resulting collective and complex interaction that helped catalyze my evolving ideas to the present form.

References

Baranger, M. (2000) *Chaos, Complexity, and Entropy: A physics talk for non-physicsts*, URL = <http://necsi.org/projects/baranger/cce.pdf>.

Callen, H. B. (1985) *Thermodynamics and Introduction to Thermostatics* John Wiley and Sons.

Callender, C. (1999) Reducing Thermodynamics to Statistical Mechanics: The Case of Entropy. *Jour. Philosophy* **96**, 348–373.

Goldstein, S. and Lebowitz, J. L. (2004) On the (Boltzmann) Entropy of Non-Equilibrium Systems. *Physica D* **193**, 53–66.

Katchalsky, A. and Curran, P. F. (1965) *Nonequilibrium Thermodynamics in Biophysics* Harvard University Press, Massachusetts.

Kondepudi, D. K. and Prigogine, I. (1998) *Modern Thermodynamics* John Wiley & Sons, Chichester.

Lebowitz, J. L. (1999) Microscopic Origins of Irreversible Macroscopic Behaviour. *Physica A* **263**, 516–527.

Nagashima, H. and Baba, Y. (1999) *Introduction to Chaos* Institute of Physics Publishing, Bristol.

Price, H. (2004) On the Origins of the Arrow of Time: Why There is Still a Puzzle about the Low Entropy Past In *Contemporary Debates in Philosophy of Science*, ed. C. Hitchcock, Blackwell.

Sengupta, A. (2003) Toward a Theory of Chaos. *International Journal of Bifurcation and Chaos* **13**, 3147–3233.

Sklar, L. (1993) *Physics and Chance: Philosophical Issues in the Foundations of Statistical Mechanics* Cambridge University Press, New York.

Uffink, J. (2001) Bluff your way in the Second Law of Thermodynamics. *Stud. Hist. Phil. Mod. Phys.* **32**, 305–394.